

CHALMERS



Activation of methane in presence of nitrogen oxides

Methane oxidation and lean NO_x reduction

Master of Science Thesis

ANDREAS PERSSON

Department of Chemical and Biological Engineering
Competence Centre for Catalysis
CHALMERS UNIVERSITY OF TECHNOLOGY
Gothenburg, Sweden, 2013

Thesis for the degree of Master of Science

Activation of methane in presence of nitrogen oxides

Methane oxidation and lean NO_x reduction

Andreas Persson

Department of Chemical and Biological Engineering
Competence Centre for Catalysis
CHALMERS UNIVERSITY OF TECHNOLOGY
Göteborg, Sweden 2013

Abstract

To preserve our nature, new sustainable fuels are needed. One of the proposed new fuels is biogas, which mainly contains methane. However, also the use of methane as fuel needs environmental considerations. First is the fact that methane is a strong greenhouse gas, which means that non-reacted methane in the exhaust gases has to be dealt with by oxidizing it to carbon dioxide, which compared to methane has a much lower climate impact. This is easiest done by the use of catalysts. Preferably these catalysts would at the same time be able to reduce NO_x present in the exhaust. Therefore, this project has focused on catalysts potentially capable of both oxidation of methane and reduction of NO_x simultaneously.

Four catalysts were prepared and tested; Pt/In/Al₂O₃, Pt/ Al₂O₃, Pt/In/ZSM-5 and Pt/ZSM-5. They were first tested in a gas flow reactor with temperature varied between 50^oC and 550^oC, with NO_x either present or absent. The Pt/In/Al₂O₃, Pt/ Al₂O₃, and Pt/ZSM-5 catalysts were then further evaluated in a gas flow reactor experiment, now with NO_x varied with time in pulses, at 250^oC, 300^oC and 400^oC.

Neither of the studied catalysts appeared to be able to reduce the NO_x, though all were able to oxidize methane to various levels. The Pt/ZSM-5 catalyst had the lowest conversion, while the Pt/In/Al₂O₃ catalyst had the highest. The two catalysts without Indium achieved results between the other two.

Contents

1. Introduction	5
1.1 Objective of the project	5
2. Theoretical background.....	5
2.1. Catalysis.....	6
2.1.1 The Catalytic cycle.....	6
2.2. Sol-gel method of catalyst preparation	8
2.3. Fourier Transform Infrared (FTIR) Spectroscopy	8
3. Experimental procedure	9
3.1. Preparation of catalysts.....	9
3.1.1. Indium/alumina catalyst.....	10
3.1.2. Indium/zeolite catalyst	10
3.1.3. Palladium addition	10
3.1.4. Monolith coating	10
3.2. Flow reactor experiments	10
3.2.1. Evaluation of CH ₄ oxidation and NO _x reduction	10
3.2.2. Transient pulse experiment	11
4. Results and discussion.....	12
4.1. Evaluation of CH ₄ oxidation and NO _x reduction	13
4.2. Transient reactor experiments	18
5. Conclusions	22
6. Future Work	23
7. Acknowledgements	23
Appendix A: Gas concentration graphs for evaluation experiment	24
Appendix A1.1: CH ₄ concentration over Pd/In/Al ₂ O ₃ catalyst	24
Appendix A1.2: CO ₂ concentration over Pd/In/Al ₂ O ₃ catalyst	24
Appendix A1.3: NO concentration over Pd/In/Al ₂ O ₃ catalyst	25
Appendix A1.4: NO ₂ concentration over Pd/In/Al ₂ O ₃ catalyst.....	25
Appendix A1.5: Total NO _x concentration over Pd/In/Al ₂ O ₃ catalyst.....	26
Appendix A2.1 CH ₄ concentration over Pd/Al ₂ O ₃ catalyst.....	26
Appendix A2.2: CO ₂ concentration over Pd/Al ₂ O ₃ catalyst.....	27
Appendix A2.3: NO concentration over Pd/Al ₂ O ₃ catalyst.....	27
Appendix A2.4: NO ₂ concentration over Pd/Al ₂ O ₃ catalyst	28

Appendix A2.5: Total NO _x concentration over Pd/Al ₂ O ₃ catalyst	28
Appendix A3.1 CH ₄ concentration over Pd/ZSM-5 catalyst.....	29
Appendix A3.2: CO ₂ concentration over Pd/ZSM-5 catalyst.....	29
Appendix A3.3: NO concentration over Pd/ZSM-5 catalyst.....	30
Appendix A3.4: NO ₂ concentration over Pd/ZSM-5 catalyst	30
Appendix A3.5: Total NO _x concentration over Pd/ZSM-5 catalyst	31
Appendix A4.1 CH ₄ concentration over Pd/In/ZSM-5 catalyst	31
Appendix A4.2: CO ₂ concentration over Pd/In/ZSM-5 catalyst	32
Appendix A4.3: NO concentration over Pd/In/ZSM-5 catalyst	32
Appendix A4.4: NO ₂ concentration over Pd/In/ZSM-5 catalyst.....	33
Appendix A4.5: Total NO _x concentration over Pd/In/ZSM-5 catalyst.....	33
Appendix B: Gas concentration graphs for transient pulse experiment.....	34
Appendix B1.1: CH ₄ gas concentration graphs for 50% NO over all catalysts at all temperatures.....	34
Appendix B1.2: NO _x gas concentration graphs for 50% NO over all catalysts at all temperatures.....	35
Appendix B2.1: CH ₄ , CO ₂ and NO _x gas concentration graphs for all NO concentration over Pd/In/Al ₂ O ₃ catalyst at 300 ^o C	36
Appendix B2.2: CH ₄ , CO ₂ and NO _x gas concentration graphs for all NO concentration over Pd/In/Al ₂ O ₃ catalyst at 400 ^o C	37
Appendix B3.1: CH ₄ , CO ₂ and NO _x gas concentration graphs for all NO concentration over Pd/Al ₂ O ₃ catalyst at 300 ^o C.....	38
Appendix B3.2: CH ₄ , CO ₂ and NO _x gas concentration graphs for all NO concentration over Pd/Al ₂ O ₃ catalyst at 400 ^o C.....	39
Appendix B4.1: CH ₄ , CO ₂ and NO _x gas concentration graphs for all NO concentration over Pd/ZSM-5 catalyst at 300 ^o C.....	40
Appendix B4.2: CH ₄ , CO ₂ and NO _x gas concentration graphs for all NO concentration over Pd/ZSM-5 catalyst at 400 ^o C.....	41

1. Introduction

The global climate change has put emphasis on emission of CO₂, not least due to exhaust gases from cars, trucks and other vehicles driven by combustion engines. This calls for more efficient combustion, such as diesel- and lean-burn engines, which are run in excess oxygen. Furthermore combustion engines emit CO due to incomplete combustion and NO_x, created in the combustion as well as emissions of unburned fuel. The usual way of treating the exhausts from stoichiometric engines is by use of three-way catalytic (TWC) converters, allowing for both oxidation of remaining hydrocarbons and CO, as well as reduction of NO_x. However, the lean environment obstructs the NO_x reduction in the TWC, which puts new demands on the NO_x abatement techniques. [Maunula, T; Ahola, J; Hamada H; (2007), Reaction Mechanism and Microkinetic Model for the Binary Catalyst Combination of In/ZSM-5 and Pt/Al₂O₃ for NO_x Reduction by Methane under Lean Conditions, Industrial & Engineering Chemistry Research, 46, 2715-2725.]

Together with energy efficient combustion engines, sustainable fuels will most likely contribute to a significant reduction of the CO₂ emissions. One such possible fuel is biogas, which mainly contains methane.

Even though methane can be derived from renewable resources, it is by itself a very strong greenhouse gas, meaning that unreacted methane released with the exhausts will have a major impact on the environment. Therefore, catalytic conversion will be needed not only to reduce the NO_x produced by a methane-driven engine, but also for oxidation of methane in the exhaust gases. Since methane is a very stable molecule, especially in the conditions that would be prevalent in exhaust gases, finding suitable catalysts will not only be important, but also tricky and probably require a lot of scientific study and experimentation. [Maunula, T; Ahola, J; Hamada H; (2007), Reaction Mechanism and Microkinetic Model for the Binary Catalyst Combination of In/ZSM-5 and Pt/Al₂O₃ for NO_x Reduction by Methane under Lean Conditions, Industrial & Engineering Chemistry Research, 46, 2715-2725.]

Preferably, a single catalyst could be found that is able to catalyze both the oxidation of methane (and CO) and the reduction of NO_x.

1.1 Objective of the project

The objective of this master thesis project is to investigate suitable catalysts for oxidation of CH₄ in an atmosphere similar to that expected in exhaust gases from energy-efficient engines, with an excess of O₂. The work focuses on methane oxidation in presence and absence of NO_x, preferably oxidizing methane and reducing NO_x simultaneously.

2. Theoretical background

A basic understanding of catalysis might be needed to understand all aspects of this master thesis, and is therefore provided. The sol-gel method of catalyst preparation is a commonly used method, which is used this project. Finally, gas analysis was performed by use of Fourier Transform Infrared Spectroscopy and thus deserves a mention.

2.1. Catalysis

Catalysts are defined as substances that influence the reaction rate of a chemical reaction, without altering the overall reaction itself and without being consumed by it. The thermodynamics remain unchanged, since the overall reaction itself is unchanged, and thus the chemical equilibrium is unaffected, and reactions that are impossible, and not only very slow, remain so even with an added catalyst.

Catalysis can be either homogeneous, meaning that the catalyst is in the same phase as the reactants, or heterogeneous, when the catalyst and the reactants/products are in different phases. The experiments done in this master thesis were done with heterogeneous catalysts (with gas phase reactants, and products, over a solid state catalyst), and therefore, more focus will be on this type. [Bowker, M., *The Basis and Applications of Heterogeneous Catalysis*, 4th edition, 1998, Oxford Science Publications]

2.1.1 The Catalytic cycle

The heterogeneous catalytic process includes a number of different stages that differentiates it from a normal reaction in gas phase. This can be described as a catalytic cycle, as the catalyst itself is unaffected by the reaction and indistinguishable from how it looked before the reaction took place. This can be either because the catalyst itself barely participates aside from providing a surface, or it can be because the catalyst is regenerated at the end of the cycle. The stages of this cycle are illustrated in Figure 1.

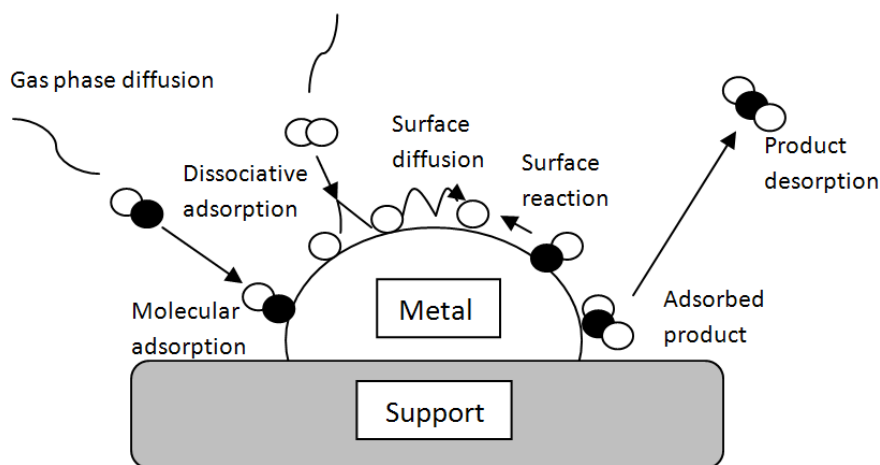


Figure 1: The stages that can be involved in reactions on a supported catalyst, illustrated by oxidation of carbon monoxide to carbon dioxide. [Bowker, M., *The Basis and Applications of Heterogeneous Catalysis*, 4th edition, 1998, Oxford Science Publications]

The reaction starts with the reactants being adsorbed onto the catalyst. This can either be molecular adsorption, when the reactants remain intact on the catalyst surface, or it can be dissociative adsorption, when the reactant molecule is split into several fragments of one or more atoms. These reactants are not statically bound to the surface and may diffuse along it. The reactants will then be able to react relatively easily and form an adsorbed product, which finally desorbs from the catalyst surface.

The increased activity on the surface of the catalyst is owing to this surface constituting a relatively abrupt termination of the properties of the material and thus providing free valence electrons. These valence electrons will then provide formation of new chemical bonds between the atom/molecule and the catalyst surface and will allow it to react with other molecules/atoms on the surface.

Naturally, a larger surface area is (almost) always preferable with catalysts, since it will increase the amount of free bonds for reactants to adhere to. What material the catalyst is made of is also important, since different materials has different properties, both in the bulk and on the surface. Materials like noble metals, metals and metal oxides all can act as catalysts for various purposes.

Often the active material is dispersed onto a support structure. This is mainly for two reasons. Primary factor is cost. Many catalytic materials, such as platinum, are expensive and making a catalyst out of just the active part would be economically unfeasible. At the same time, these catalytic materials are often metals, or metal complexes, with a tendency to agglomerate when under heating, and thereby reducing the active surface area. By having a support of a different material, both cheaper and less prone to agglomeration, it is possible to provide a relatively cheap catalyst with a large surface area. This support can either be inert, or it may participate in the catalytic reaction in some way, e.g. by altering the catalytic properties of the material or by providing new catalytic sites.

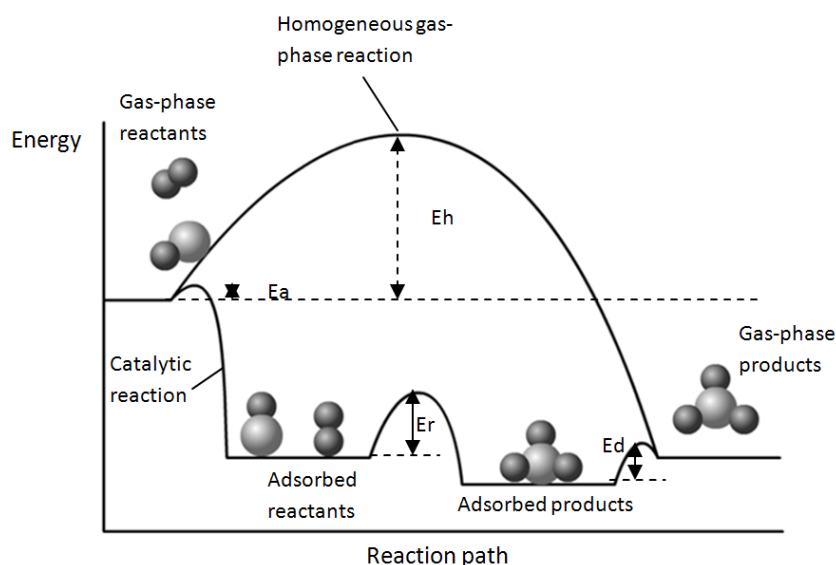


Figure 2: The energy barriers involved in uncatalyzed and catalyzed reactions. E_h = activation energy of uncatalyzed reaction, E_a = activation energy of adsorption, E_r = activation energy of catalyzed reaction (of adsorbed species), E_d = activation energy of desorption. [Bowker, M., *The Basis and Applications of Heterogeneous Catalysis*, 4th edition, 1998, Oxford Science Publications]

Figure 2 shows the difference in activation energies between a catalyzed reaction and the same reaction in gas phase. The activation energy for the gas phase reaction is large mainly

because of the intermediate product, with several unfilled valences. The similar intermediate product in the catalyzed reaction avoids this by being loosely bonded to the catalyst surface, sharing the electrons with the surface, thereby substantially reducing the activation energy. The stages shown in figure 1 are clearly present. However, molecular and dissociative adsorptions are not being differentiated. [Bowker, M., *The Basis and Applications of Heterogeneous Catalysis*, 4th edition, 1998, Oxford Science Publications]

2.2. Sol-gel method of catalyst preparation

The sol-gel method is used for fabrication of various metals and metal oxides, among them catalysts and catalyst supports. It differs from other catalytic preparation methods, such as wet impregnation, in that the catalytic particles can be made a part of the manufacturing process, with smaller sizing and more evenly spread throughout the support, with lesser probability of agglomeration. At the same time, the method allows production of materials with a high purity and greater homogeneity than usual by other means. [Hench, L. L; West, J. K; (1990), *The Sol-Gel Process*, *Chemical Reviews*, 90, 33-72.]

The sol-gel method is initiated by adding the precursors (in this project, aluminum isopropoxide (AIP) to form Al_2O_3) needed, as well as any additions (such as catalytic materials) into an excess of solvent, usually water. At this stage, it is possible to make additions, such as changing the pH, to vary the structure of the final product. The sol is kept steady, with the particles dispersed and avoiding sedimentation due to the Brownian motion of the solvent.

The solvent is slowly removed, usually in conditions not too far from room temperature, the solvent instead being removed by lowered pressure. As the solvent is removed, the solid particles begin to grow in ordered structures while still being kept apart by water molecules, initially only a few particles wide. When more solvent is removed, these structures will converge and interact with each other until reaching a point where they're no longer separate entities but a homogenous lattice. Once this point has been reached throughout the sample, a gel is said to be formed. [H. Kannisto; (2010), *Lean NOx reduction over silver-alumina catalysts*, Department of Chemical and Biological Engineering, Chalmers University of Technology.]

Removing the last of the solvent from the gel can be troublesome, especially if one wants it to keep the structure that has formed. By avoiding the solid-liquid interface, for example by freeze-drying the sample, allows this structure to be preserved with a minimum of difficulties. As the solvent is removed, the structure is shrunk, but the general shape of it remains, including the large surface area/weight ratio.

Finally, the sample is preferentially heat-treated, usually by calcination, to stabilize it and deactivate unreacted precursors. [Hench, L. L; West, J. K; (1990), *The Sol-Gel Process*, *Chemical Reviews*, 90, 33-72.]

2.3. Fourier Transform Infrared (FTIR) Spectroscopy

FTIR works by exposing the sample to infrared radiation. The sample will then absorb certain wavelengths and transmit others, depending on the molecules of the sample and the vibration

frequencies between these. These absorbed/transmitted wavelengths are characteristic for each molecule, providing a fingerprint for each molecule, and thus the composition of the sample. This technique is able to provide both a qualitative analysis, answering “what is in the sample”, as well as a quantitative analysis (how much is in the sample) by the size of the absorption peaks. It is, however a requirement of the molecules that are to be detected that they must have a dipole moment, meaning that while e.g. NO and CO₂ can be detected, O₂ and N₂ cannot.

An interferometer is used before the IR beam is exposed to the sample to be able to measure all frequencies at the same time, by using a beam splitter to separate the incoming beam and then recombining it, when the two parts have travelled slightly different distances. The resulting beam will then interfere with itself, which results in an interferogram, where each data point has information about every IR frequency from the source.

The signal is Fourier transformed into a frequency spectra for the analysis, which at the same time allows for precise and quick measurements.

Due to absorption intensity being a relative value, a background spectra is needed, which at the same time removes any interference from the instrument itself. [Thermo Nicolet Corporation, (2001), Introduction to Fourier Transform Infrared Spectrometry, <http://mmrc.caltech.edu/FTIR/FTIRintro.pdf> [visited 2011-12-12].]

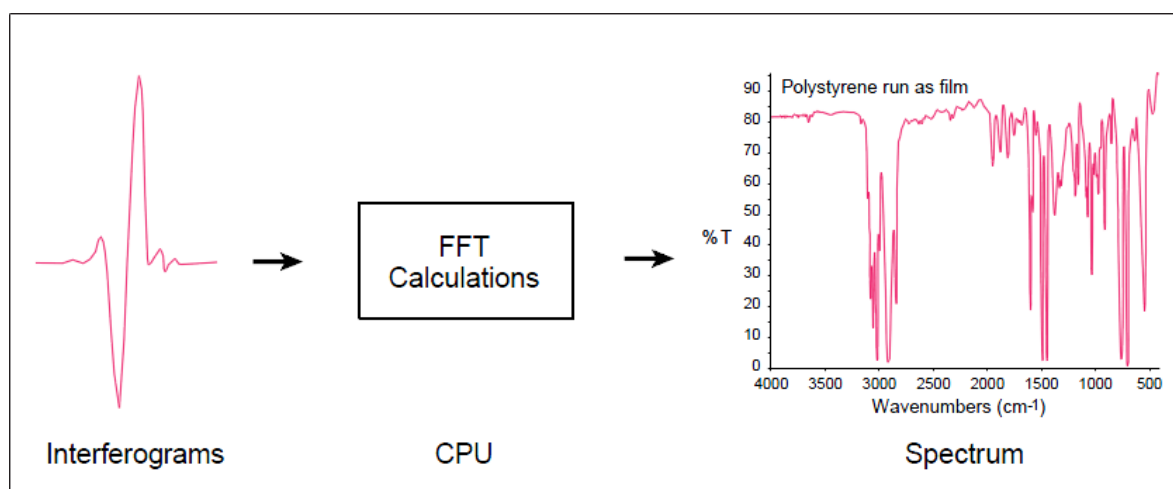


Figure 3: Basic principle behind FTIR spectroscopy. [Thermo Nicolet Corporation, (2001), Introduction to Fourier Transform Infrared Spectrometry, <http://mmrc.caltech.edu/FTIR/FTIRintro.pdf> [visited 2011-12-12].]

3. Experimental procedure

3.1. Preparation of catalysts

Four different catalysts were made, Pd/In/ZSM-5, Pd/ZSM-5, Pd/In/Al₂O₃ and Pd/Al₂O₃. The zeolite, (ZSM-5), and alumina (Al₂O₃) support materials were obtained from commercially

available sources with no alterations except calcination (550-600°C, 1h). The indium was initially applied, with ion exchange methods for the Pd/In/ZSM-5 and with a sol-gel method for the Pd/In/ Al₂O₃. After that, Pd was applied with incipient wetness impregnation, and the catalysts were finally coated on a monolith for the flow reactor experiments.

3.1.1. Indium/alumina catalyst

The In/Al₂O₃ catalyst was prepared by dissolving 19 g aluminum isopropoxide (AIP) in 400 ml milli-Q water. Once an even dispersion had been obtained, 0,26 g of indium nitrate hydrate (In(NO₃)₃*3H₂O) was added in 20 ml milli-Q water and poured into the solution as it was stirred. This was heated to 80°C, and 10% HNO₃ was added until the solution cleared and a sol was formed. The sol was continuously stirred until it had cooled to room temperature. The solvent was partially removed in reduced pressure until a gel formed, which was then freeze dried overnight. Finally, it was calcined for 3 h at 550°C.

3.1.2. Indium/zeolite catalyst

The In/ZSM-5 catalyst was prepared by dissolving 0,38 g indium nitrate hydrate in 1000 ml milli-Q water and adding 4,75 g H-ZSM-5. This was then heated to 85°C and kept stirred for 7 hours. After that, the solution was filtered and washed, and the catalyst, in the filter cake, kept slightly damp. The process was repeated twice, and the catalyst was finally allowed to dry out. Finally, the catalyst was calcined for 3 h at 550°C.

3.1.3. Palladium addition

The final palladium coating of the catalysts were performed by adding 2 g of 7,53 weight% palladium nitrate solution, further diluted with milli-Q water to 4,85 g catalyst/support. This was stirred vigorously, until an even coating had been achieved. The catalysts were freeze-dried and calcined for 1h at 550°C.

3.1.4. Monolith coating

The catalytic materials were coated onto monolithic structures by mixing 3 g catalyst, 0.75 g binder and 15 g water into a slurry. The monoliths were then dipped in this slurry, slowly dried at 95°C for 5 minutes and then calcined at 600°C for 2-3 minutes. This procedure was repeated until a total mass of 1 g catalyst had been applied onto each monolith. The monoliths were then finally calcined at 550°C for 1h.

3.2. Flow reactor experiments

The flow reactor experiments were performed in a heated gas flow reactor. To achieve an even temperature of the catalyst, additional monoliths were placed in front of and behind the catalyst monolith, and the gas flowing through it was heated for roughly 0,5 m before entering the monoliths. The outlet gases were analyzed with FTIR.

3.2.1. Evaluation of CH₄ oxidation and NO_x reduction

To provide a quick evaluation of the CH₄ oxidation and NO_x reduction performance for the different catalysts in a range of temperatures, extinction/ignition experiments were performed in a gas flow reactor. This was done both with and without NO_x present in the system, to facilitate comparison of the catalysts and how they were affected by the NO_x.

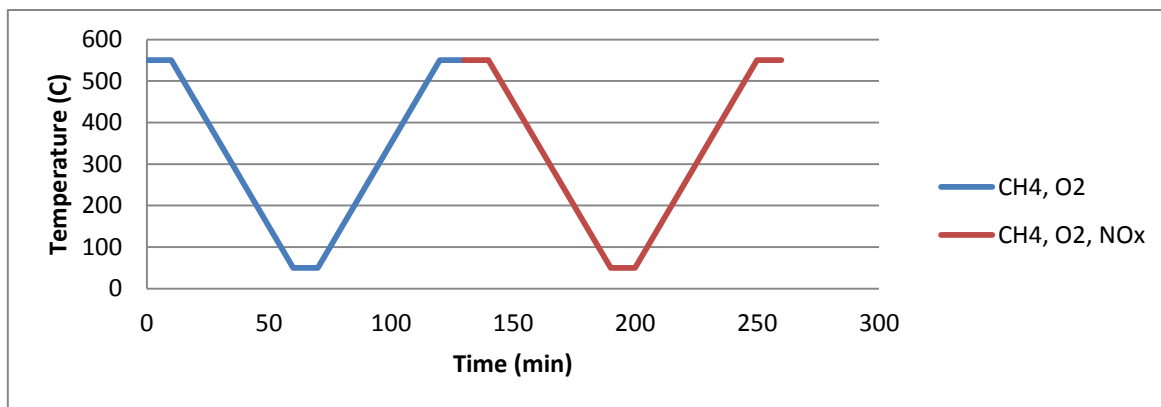


Figure 3: The evaluation experiment as planned, showing how the temperature and gas composition was varied with time.

Each catalyst was run through the same schedule consisting of first 70 min of 0,1% CH₄ and 1% O₂ in Ar gas flow, and a total gas flow of 3500 ml/min, at 550^oC, to burn away organic contamination and achieve a steady state. The temperature was then lowered, by 10^oC/min, to 50^oC, with the gas flow constant. After a 10 min stabilization period at 50^oC, the temperature was increased, by 10^oC/min, back to 550^oC. After another 10 min stabilization period, the gas flow composition was changed to 0,1% CH₄, 0,9% O₂, 0,1% NO and 0,05% NO₂. This was then given a 10 min stabilization period, and then the temperature was lowered to 500^oC, by 10^oC/min. Another 10 min stabilization period and the temperature were raised, once more by 10^oC/min, to 550^oC. After a final 10 min stabilization period, the experiment was concluded, the gas flow was shut off and the catalyst allowed to cool down.

3.2.2. Transient pulse experiment

For a more complete evaluation of the most promising catalysts, Pd/In/Al₂O₃, Pd/Al₂O₃ and Pd/ZSM-5, these were run in the gas flow reactor at a constant temperature in an atmosphere of O₂ and CH₄ and Ar as balance, as NO_x was pulsed through in four pulses and the response was studied. This was done for several different NO_x compositions and three different temperatures were it was estimated from the previous experiment that all catalysts were active. These temperatures were chosen to 250, 300 and 400^oC.

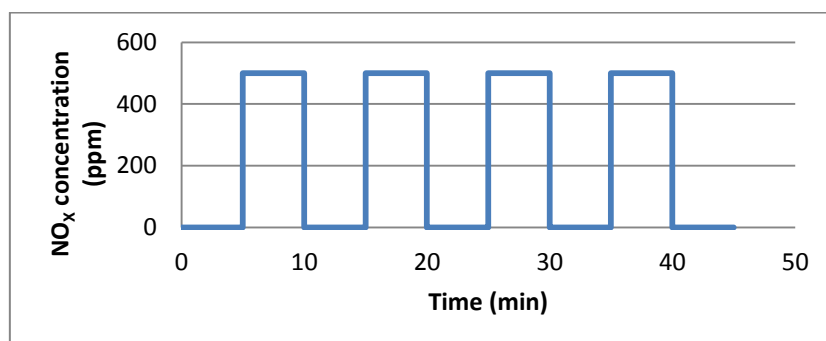


Figure 4: The NO_x pulses in the transient pulse experiment as they were varied with time

Table 1

Summary of the experimental conditions for the pulse experiment.

Experiment/pulse	Gas composition	Duration	Process
Init	1,0 vol% O ₂ /0,1 vol% CH ₄ /Ar	30 min	Stabilisation, initiation
P100	1,0 vol% O ₂ /0,1 vol% CH ₄ /0,05 vol% NO ₂ /Ar	5 min	NO _x pulse
	1,0 vol% O ₂ /0,1 vol% CH ₄ /Ar	5 min	Desorption
P75	1,0 vol% O ₂ /0,1 vol% CH ₄ /0,0125 vol% NO/0,0375 vol% NO ₂ /Ar	5 min	NO _x pulse
	1,0 vol% O ₂ /0,1 vol% CH ₄ /Ar	5 min	Desorption
P50	1,0 vol% O ₂ /0,1 vol% CH ₄ /0,025 vol% NO/0,025 vol% NO ₂ /Ar	5 min	NO _x pulse
	1,0 vol% O ₂ /0,1 vol% CH ₄ /Ar	5 min	Desorption
P25	1,0 vol% O ₂ /0,1 vol% CH ₄ /0,0375 vol% NO/0,0125 vol% NO ₂ /Ar	5 min	NO _x pulse
	1,0 vol% O ₂ /0,1 vol% CH ₄ /Ar	5 min	Desorption
P0	1,0 vol% O ₂ /0,1 vol% CH ₄ /0,05 vol% NO/Ar	5 min	NO _x pulse
	1,0 vol% O ₂ /0,1 vol% CH ₄ /Ar	5 min	Desorption

Each pulse P0, P25, P50, P75 and P100 was repeated four times after each other. Init was performed before the first pulse in P0, P75 and P100. The experiments were repeated for 250, 300 and 400°C.

A total flow of 3500 ml/min of gas was utilized, with Ar as the main component. The gas flow also consisted of 1% O₂ and 0,1% CH₄, and a total concentration of 500 ppm NO_x was used in the pulses. In total, five different tests were done, with pure NO₂ in the pulses, with pure NO and with mixtures of NO and NO₂, consisting of 25, 50 and 75 % NO₂. Before the first, second and third pulse-series, the system was stabilized with a 30 min burn period, with only the O₂ and CH₄ present. Each series of pulses consisted of four pulses, each 5 min long with a 5 min pause between each. See Figure 4 and Table 1 for more details of the pulse sequences.

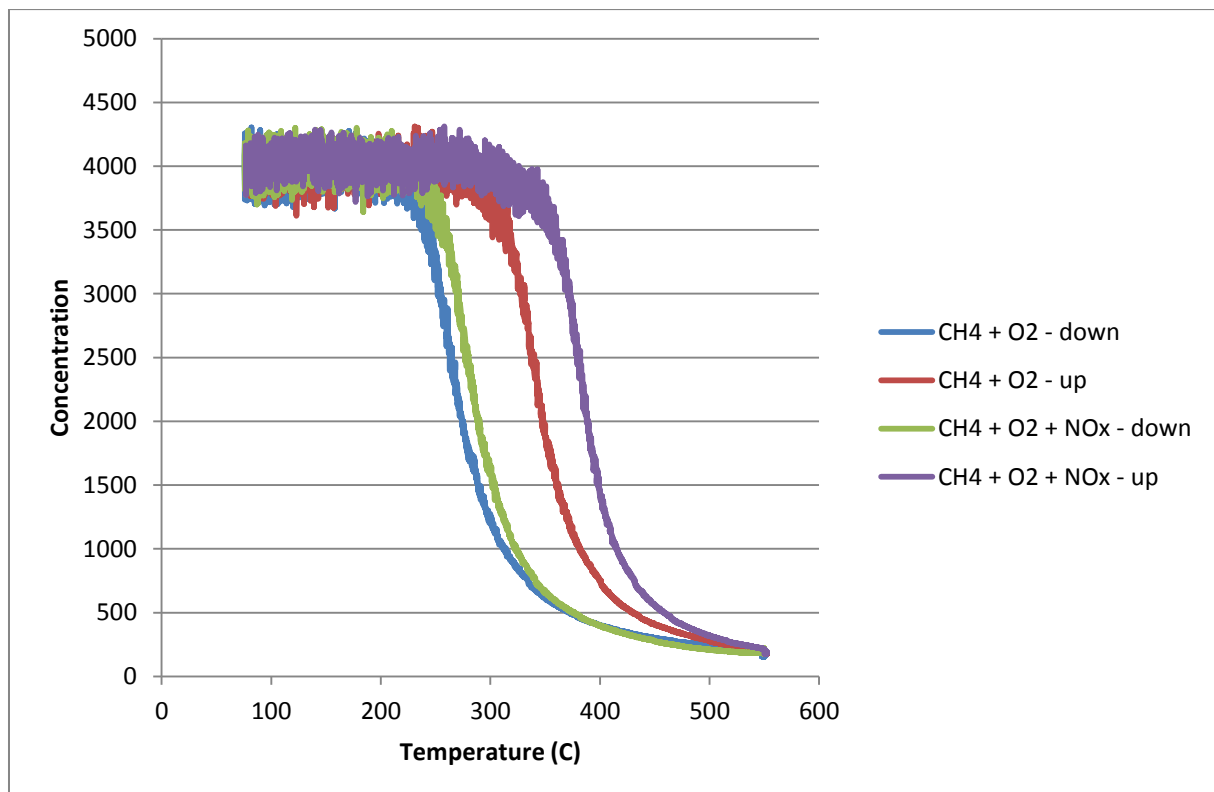
4. Results and discussion

The idea behind the experiments was to evaluate the ability of the catalysts to oxidize CH₄, while simultaneously reducing NO_x. In the end, catalysts able to oxidize CH₄ in the presence of NO_x were found, however, none of the tested samples were able to reduce the NO_x itself to a significant degree, and the CH₄ oxidation was adversely affected by the NO_x.

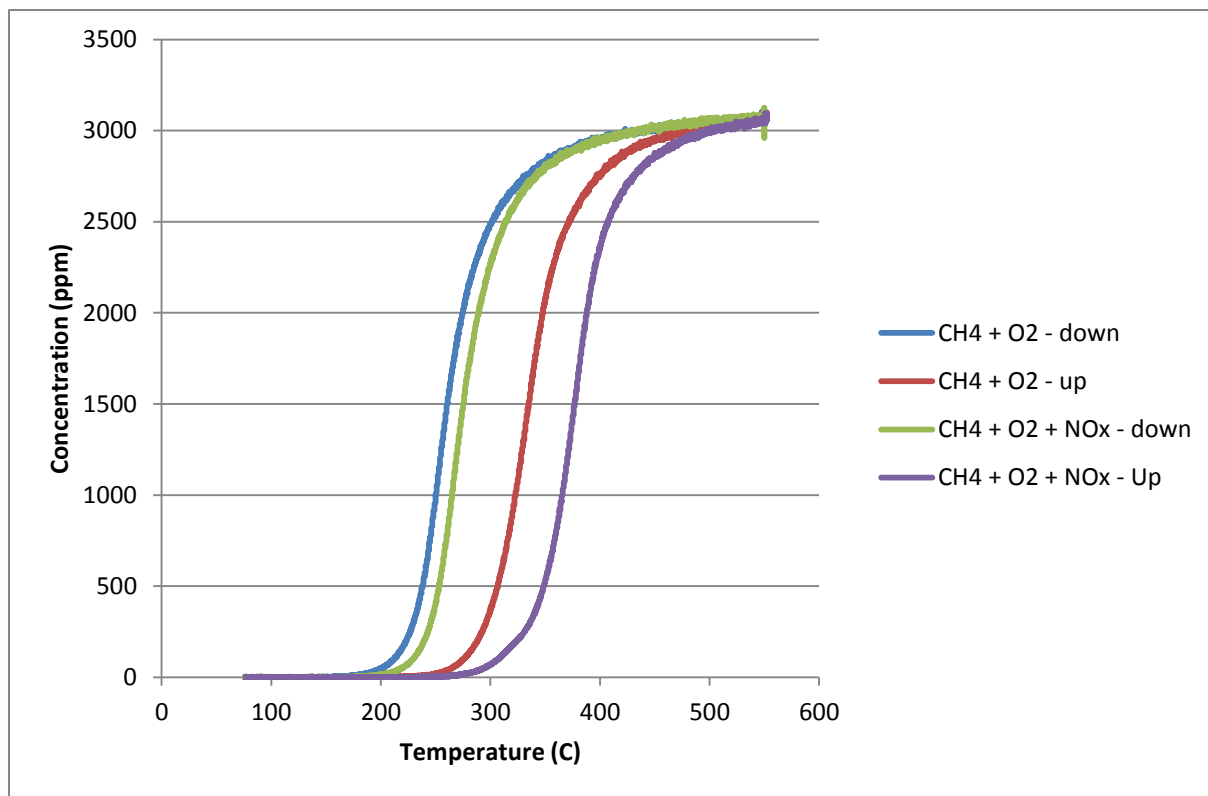
4.1. Evaluation of CH₄ oxidation and NO_x reduction

The idea behind the experiment was to study the catalyst behavior as a function of temperature, in a temperature range where all the catalysts would presumably be active (550°C) to where they would be non-activate (set to 50°C, though this temperature wasn't always reached due to slow cooling).

The gas concentrations after the reactor were plotted separately against the temperature in the reactor, and these data were then compared between the different catalysts. For all graphs, see Appendix 1. All the catalysts showed a similar behavior, though the exact temperature of deactivation varied. Throughout this chapter, when the graph for only one catalyst is shown, it will be that for Pd/In/Al₂O₃.



Graph 1: Concentration of CH₄ on Pd/In/Al₂O₃



Graph 2: Concentration of CO₂ on Pd/In/Al₂O₃

The CH₄ and CO₂ graphs, see graph 1 and 2, correspond nicely to each other, while no other possible products have been found. Of note is that roughly all CH₄ was consumed at 550^oC, while at temperatures below 200-300^oC, depending on catalyst, no reaction occur

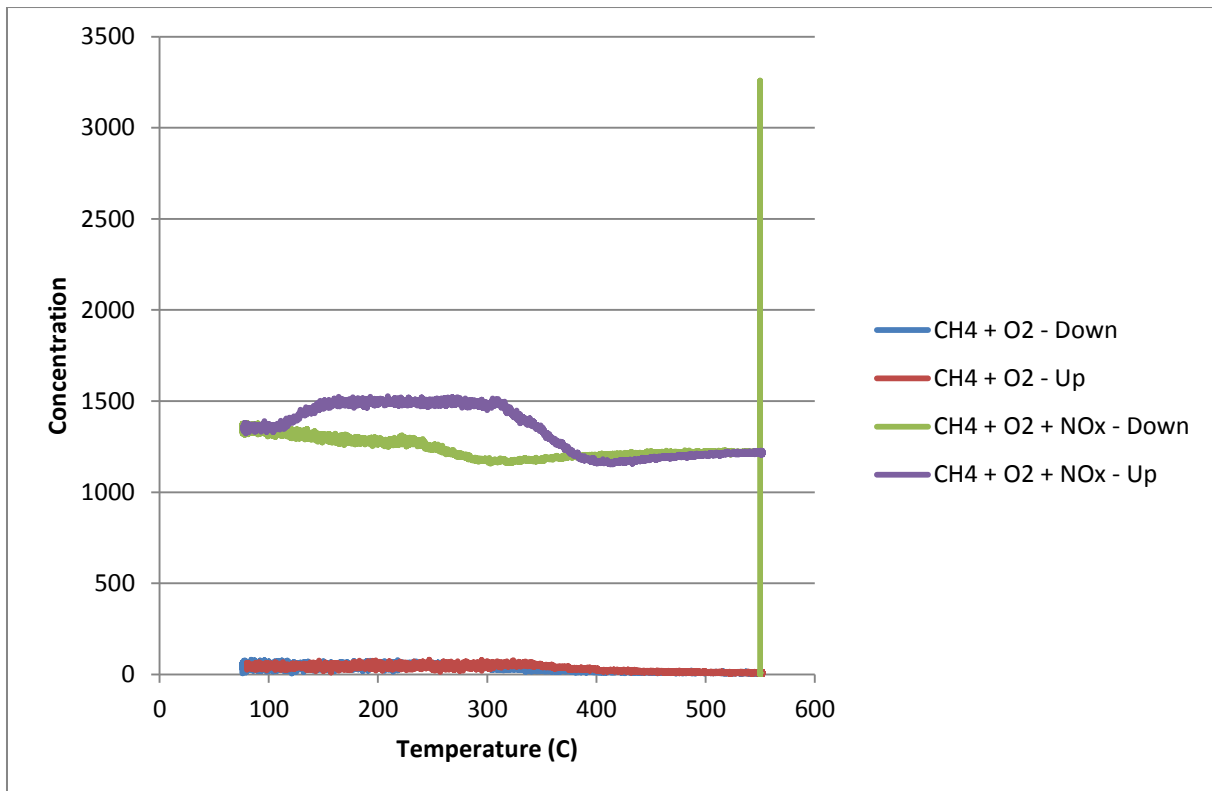
For the Pd/In/Al₂O₃ sample, the reaction run close to full conversion at 300^oC, but as the temperature is decreased, it extinguish at 200^oC. When the temperature is increased again, the ignition is delayed until roughly 250^oC is reached. When NO_x is added, the extinction occur approximately at 190^oC, while the ignition is delayed even further and also not as quick in achieving increased conversion. It can be clearly seen in the graphs that there is a very small temperature interval between “very active” and “almost inactive”, where it goes from roughly 80% conversion to almost extinguished in roughly 40^oC. None of the other catalysts showed such a steep decline in efficiency.

For the Pd/In/ZSM-5 sample, total extinction is achieved already at 300^oC, and full activity is not achieved even at 550^oC, the highest temperature in the experiment. However, the delay in igniting the reaction again is less compared to Pd/In/Al₂O₃. The ignition starts roughly 30-50^oC above the extinction temperature. Also the addition of NO_x does not affect the activity as much, and in fact seems to increase the activity, as compared to the same reaction without NO_x, when the temperature is decreased.

The Pd/Al₂O₃ catalyst also seems to not reach full conversion at 550^oC, even though the results are better than for Pd/In/ZSM-5. However, both extinction and ignition is reached at 300^oC, except for the ignition with NO_x present in the system, which is delayed to 350^oC.

Except for that, NO_x seems not to influence the system significantly, and the extinction profiles are virtually similar with and without NO_x .

Like most of the catalysts investigated here, the Pd/ZSM-5 catalyst fails to achieve full efficiency at 550°C , though it is the one with highest activity except for Pd/In/ Al_2O_3 . At 250°C , extinction is achieved without NO_x , and ignition needs about 50°C higher temperature to start. When NO_x is added, the extinction starts approximately 25°C earlier, while the ignition is severely affected and not initialized until 350°C . Even when started, it has a slower increase than in the system without NO_x .



Graph 3: Total concentration of NO_x gases on Pd/In/ Al_2O_3

The total NO_x concentration profile varies similarly for all catalysts, with a lower concentration at high temperatures, which increase as the temperature is decreased. Once the temperature is increased again, however, the concentration at first goes up further, instead of decreasing as would be expected, probably due to NO_x being adsorbed while the temperature is lowered, and then released as the temperature is increased again. Also, through all the measurements, the NO_x sequence starts with a very high flow, that soon goes down to a lower level, which then remains reasonably stable throughout the experiment. This startup increase goes beyond the concentration programmed, and might be due to a faulty valve, or some other, unknown reason.

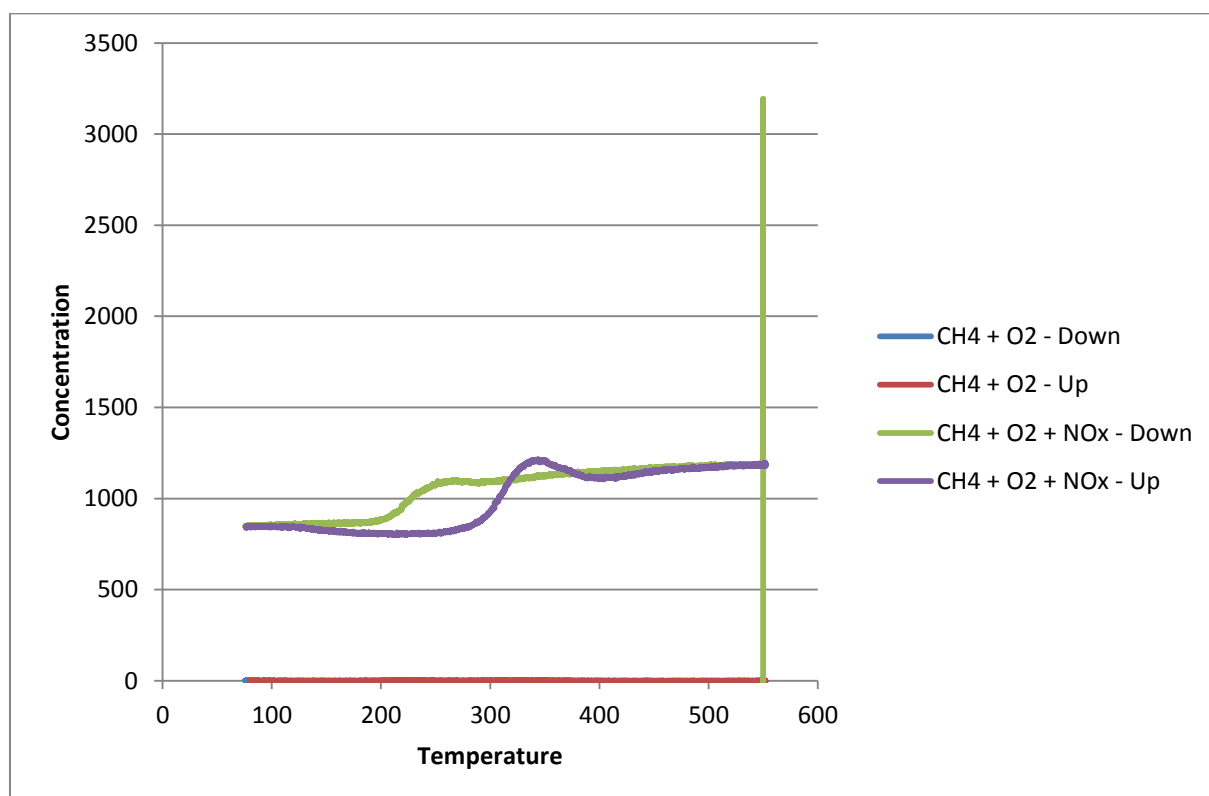
For the Pd/In/ Al_2O_3 sample, the increase in NO_x concentration is observed to begin at roughly 300°C , and has almost stabilized at 220°C , though still slowly increasing until the minimum temperature, slightly above the planned 50°C due to slow cooling, is reached. As the temperature is increased again, another increase in NO_x concentration is seen to start at

110^oC. This concentration is constant between 150^oC and 300^oC, and not until 400^oC does the concentration reach the same level as when the experiment began.

The Pd/Al₂O₃ catalyst shows almost the same behavior as the Pd/In/Al₂O₃ sample, except that the increase in NO_x concentration begins slightly earlier, at roughly 350^oC and the increase is slower.

For Pd/In/ZSM-5 the NO_x concentration begin to increase already at 400^oC, and seems to have stabilized at 250^oC, though the difference between the concentration at high and at low temperature is relatively small, in the order of perhaps 150 ppm. The “hump” seen as the temperature is increased again starts around 100^oC, reaching a maximum at 150^oC and then slowly decreasing again. Not until slightly above 400^oC does the NO_x concentration reach the same level as when the temperature decreased. However, it is generally somewhat lower than that of Pd/In/Al₂O₃.

The Pd/ZSM-5 catalyst has a somewhat more pronounced hump than the Pd/In/ZSM-5, but otherwise the two graphs are almost indistinguishable.



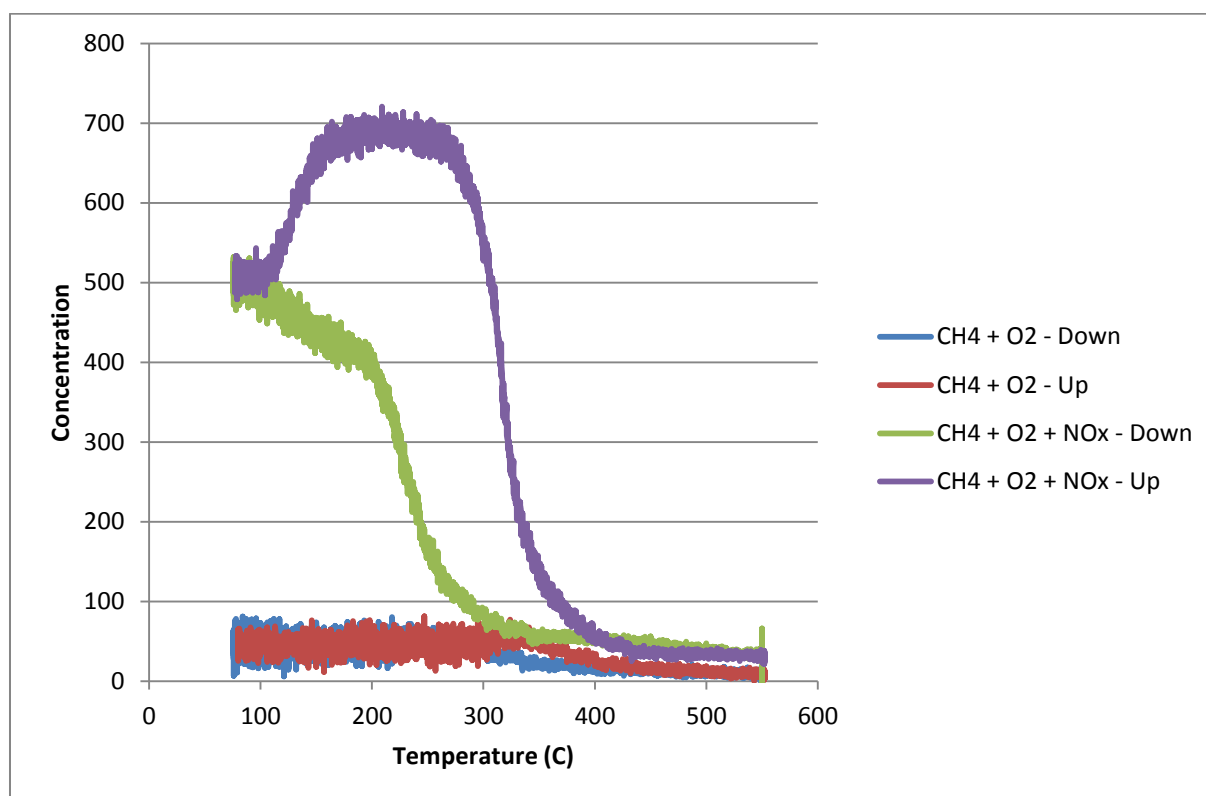
Graph 4: Concentration of NO on Pd/In/Al₂O₃

The NO graphs for Pd/In/Al₂O₃ and Pd/Al₂O₃ are not as similar as could be expected from the graphs of total NO_x. While the general shapes of the graphs are similar, the exact temperatures vary for the two samples. A similar behavior can be seen when comparing the graphs for Pd/In/ZSM-5 and Pd/ZSM-5, the general shapes are similar while the temperatures varies somewhat.

The Pd/In/Al₂O₃ catalyst shows a decrease in NO at 250^oC while cooling. The Pd/Al₂O₃ catalyst has a similar decrease already at 320^oC. This decrease is markedly less sharp for Pd/Al₂O₃, and a stable lower concentration of NO is reached at 210-220^oC for both catalysts. When the gas flow is heated, the NO flow begins to increase at 300^oC for both catalysts. The Pd/In/Al₂O₃ catalyst achieves a higher NO concentration at a lower temperature, but shows a hump between 310 and 350^oC, while Pd/Al₂O₃ has a slower but steady increase until 350^oC, where a new stable level of NO concentration is reached.

Both ZSM-5-based catalysts show a stable low concentration of NO achieved at 230^oC. Pd/ZSM-5 has a much sharper decline, starting at 300^oC, while the slower decline of Pd/In/ZSM-5 begin already at 380^oC. The increase in NO concentration begins at 300^oC for Pd/ZSM-5, and has achieved a stable concentration at 380^oC. For Pd/In/ZSM-5, the increase is delayed until 330^oC, and hasn't reached a stable concentration until 410^oC.

For all four graphs, there is a distinct peak at the beginning of the experiment, as was seen, and explained, also in the total NO_x flow graphs.



Graph 5: Concentration of NO₂ on Pd/In/Al₂O₃

As with the NO and total NO_x concentration graphs, the differences between Pd/In/Al₂O₃ and Pd/Al₂O₃, as well as between Pd/In/ZSM-5 and Pd/ZSM-5 are in the details, while the general trends of the graphs are similar.

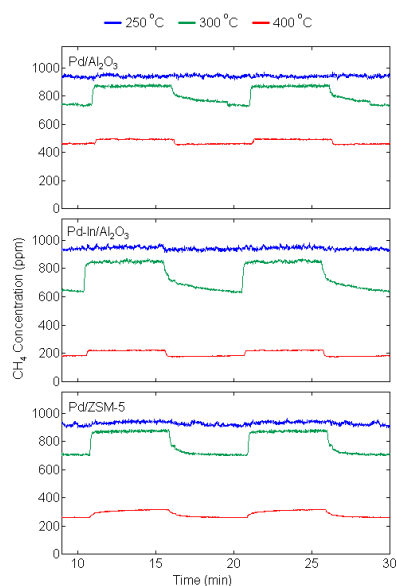
The increase in NO₂ concentration over the Pd/In/Al₂O₃ catalyst starts at 330^oC, slowing down sharply at roughly 200^oC and is still increasing at the lowest temperature. For Pd/Al₂O₃, the corresponding temperatures are 410^oC and 250^oC, respectively. When the

temperature is increased again, the NO_2 concentration at first increases further, until a maximum is reached at roughly 150-160 $^\circ\text{C}$ for both Pd/In/ Al_2O_3 and Pd/ Al_2O_3 . For Pd/In/ Al_2O_3 , the concentration decreases sharply between 300 and 350 $^\circ\text{C}$, going from almost maximum to close to minimum. The Pd/ Al_2O_3 catalyst was slower, going from close to maximum at 300 $^\circ\text{C}$ to close to minimum at 450 $^\circ\text{C}$.

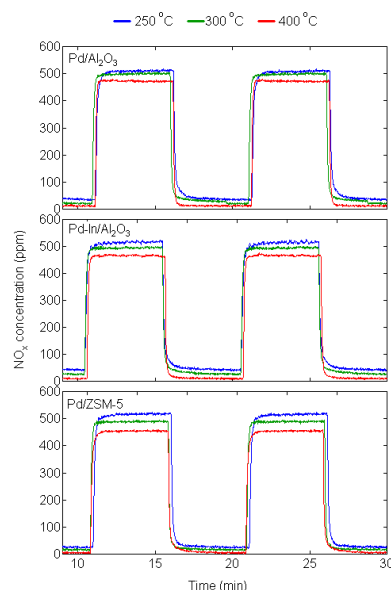
The NO_2 concentration over the Pd/In/ZSM-5 catalyst begins to increase at 400 $^\circ\text{C}$. At 260 $^\circ\text{C}$ it slows down to an almost stable level, but still rising slowly until the minimum temperature. As the temperature is increased again, a further increase in NO_2 concentration is seen at 110 $^\circ\text{C}$, reaching a maximum at 190 $^\circ\text{C}$, where after a slow decline starts. This decline accelerates at 330 $^\circ\text{C}$, and reaches close to minimum level at 450 $^\circ\text{C}$. For the Pd/ZSM-5 catalyst, the temperatures for the initial increase and final decline are 20-30 $^\circ\text{C}$ lower than for the Pd/In/ZSM-5 catalyst, but otherwise the two behave extremely similarly, including the increase in concentration as the temperature is increased, reaching maximum at 190 $^\circ\text{C}$ and then slowly declining.

4.2. Transient reactor experiments

The transient, or pulse, experiments were performed to study how transient addition of NO_x would affect the catalytic reactions, i.e. both methane oxidation and the overall NO_x reduction. As the Pd/In/ZSM-5 catalyst showed low conversion of both methane and NO_x in the temperature programmed experiments described above, this catalyst was excluded from the transient reactor experiments.

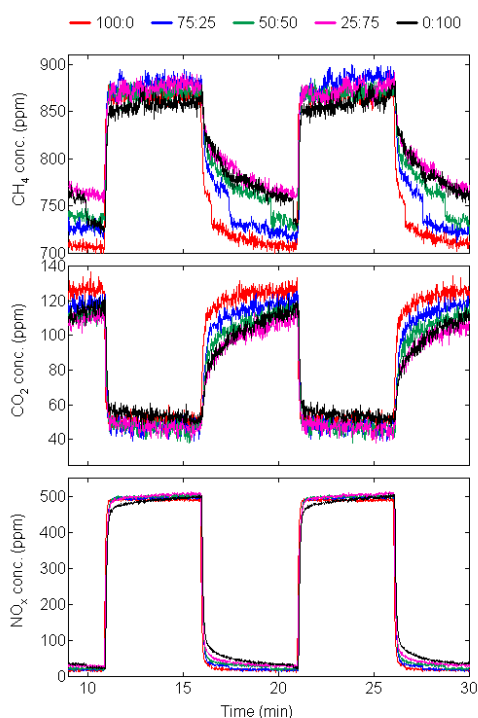


Graph 6: CH_4 concentration over all catalysts, at 250 $^\circ\text{C}$, 300 $^\circ\text{C}$ and 400 $^\circ\text{C}$, with a gas composition of 0.1% CH_4 , 1% O_2 , 500 ppm NO_x , the NO_x gas composition in turn consisting of 50% NO and 50% NO_2 .

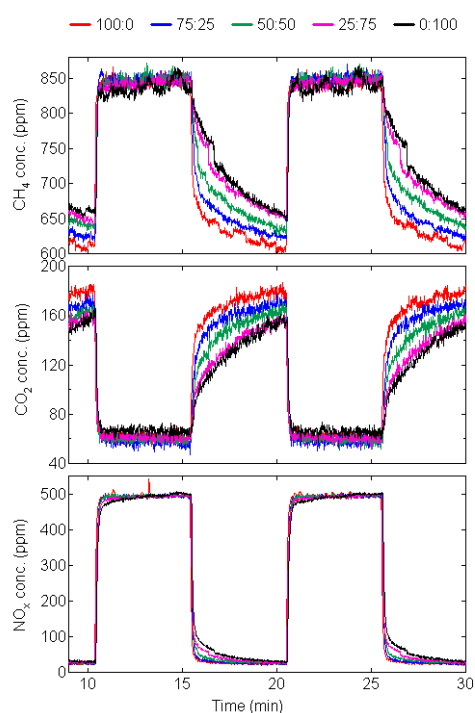


Graph 7: Total NO_x concentration over all catalysts, at 250 $^\circ\text{C}$, 300 $^\circ\text{C}$ and 400 $^\circ\text{C}$, with a gas composition of 0.1% CH_4 , 1% O_2 , 500 ppm NO_x , the NO_x gas composition in turn consisting of 50% NO and 50% NO_2 .

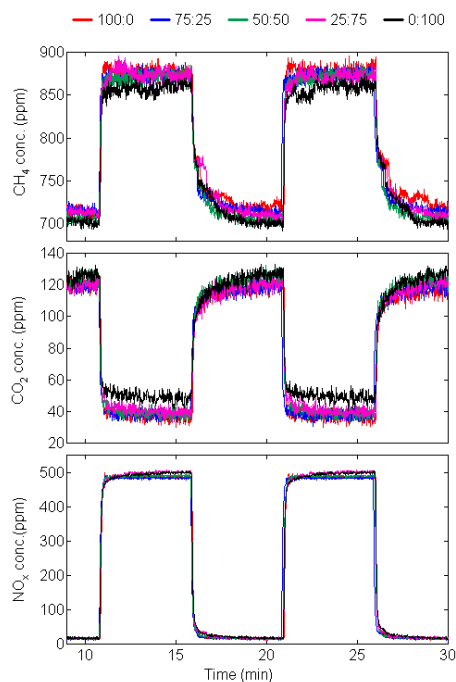
As a first comparison, the CH₄ and total NO_x concentrations were plotted for all catalysts, at all experimental temperatures, with a gas composition of 0.1% CH₄, 1% O₂, 500 ppm NO_x and Ar balance. The NO_x source consisted of 50% NO and 50% NO₂. One thing that is readily apparent in the graph is that at 250°C, there is no reaction, or almost no reaction, over any of the catalysts. In the further evaluation, this temperature can hence be ignored. 300°C and 400°C show at least some reactions taking place, and will be further studied and discussed below.



Graph 8: CH₄, CO₂ and NO_x concentrations over Pd/Al₂O₃ catalyst at 300°C, for 100% (red), 75% (blue), 50% (green), 25% (pink) and 0% (black) NO in the NO_x gas flow.



Graph 9: CH₄, CO₂ and NO_x concentrations over Pd/In/Al₂O₃ catalyst at 300°C, for 100% (red), 75% (blue), 50% (green), 25% (pink) and 0% (black) NO in the NO_x gas flow.

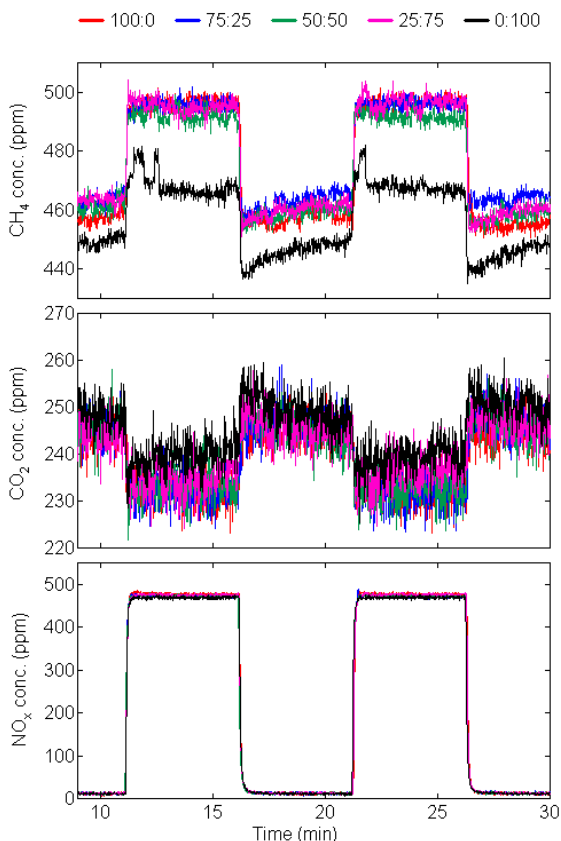


Graph 10: CH₄, CO₂ and NO_x concentrations over Pd/ZSM-5 catalyst at 300^oC, for 100% (red), 75% (blue), 50% (green), 25% (pink) and 0% (black) NO in the NO_x gas flow.

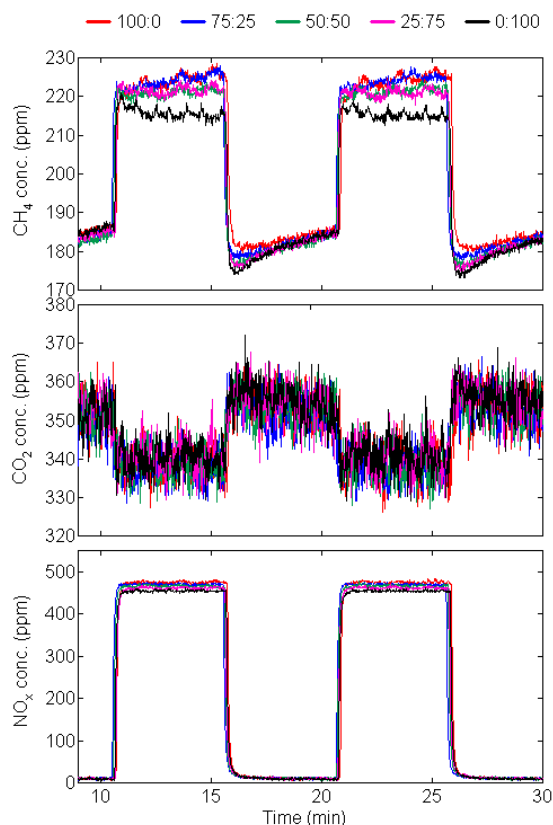
The Pd/Al₂O₃ and Pd/In/Al₂O₃ catalysts behaved roughly similar, with the CH₄ conversion being inhibited during the NO_x pulses and then being relatively slow to start up again. Pd/ZSM-5 also showed inhibited methane conversion during the NO_x pulses, but in this case, it was faster to reach the previous reaction rate after the NO_x pulse. Throughout the experiment, the Pd/In/Al₂O₃ catalyst achieved a generally higher concentration of CO₂ (and comparably lower concentration of CH₄), at 160 and 60 ppm CO₂ without and with NO_x pulsed into the system, respectively. The rate increase, on the other hand, was comparably slower than for both Pd/Al₂O₃ and Pd/ZSM-5, though it still achieved a higher total reaction rate, especially between the NO_x pulses.

Investigating the shape of the graphs, it seems plausible that NO_x is adsorbed on the catalyst surface and inhibits the methane oxidation, likely competing for the same sites as methane adsorption.

NO₂ seems to bind preferentially to the Pd/Al₂O₃ and Pd/In/Al₂O₃ catalysts, NO_x source as compared to only NO₂. The results with a mix of NO and NO₂ in the feed gas show CO₂ production to be in between these two extremes. For the Pd/ZSM-5 catalyst, NO seems to preferentially bind, since here the graph for only NO₂ shows less CO₂ than the one with only NO.

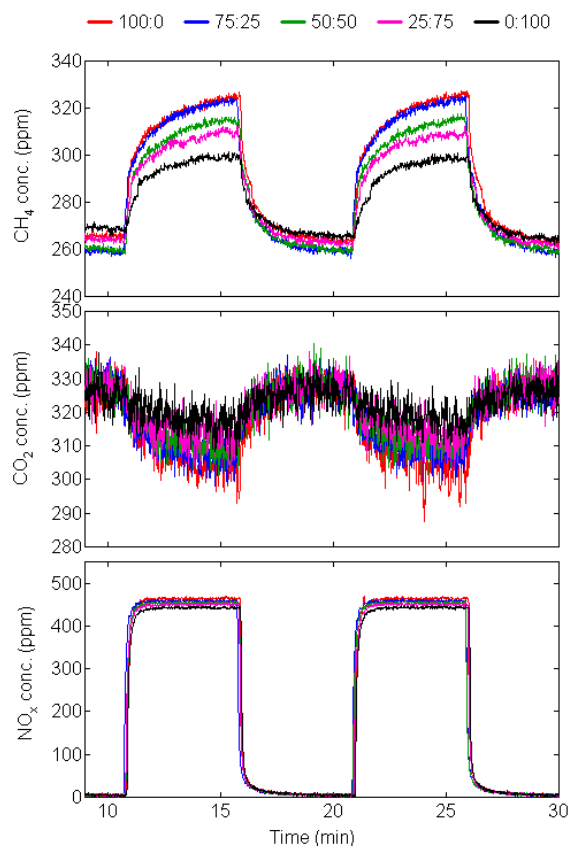


Graph 11: CH₄, CO₂ and NO_x concentrations over Pd/Al₂O₃ catalyst at 400°C, for 100% (red), 75% (blue), 50% (green), 25% (pink) and 0% (black) NO in the NO_x gas flow.



Graph 12: CH₄, CO₂ and NO_x concentrations over Pd/In/Al₂O₃ catalyst at 400°C, for 100% (red), 75% (blue), 50% (green), 25% (pink) and 0% (black) NO in the NO_x gas flow.

At 400°C, the Pd/In/Al₂O₃ and Pd/Al₂O₃ catalysts are no longer as similar. The catalyst with In has a much lower outlet concentration of CH₄, and correspondingly higher concentration of CO₂, compared to both the Pd/Al₂O₃ and the Pd/ZSM-5 catalysts. In fact, the outlet CH₄ concentration appears to be lower for the Pd/In/Al₂O₃ during the NO_x pulses than for the other catalysts between the pulses. In general, there is only a small difference between the different NO:NO₂ ratios. However, for Pd/Al₂O₃ and only NO₂, a significantly smaller increase is seen in the CH₄ outlet concentration, compared to other mixtures. Already at 25% NO, this seems to have been neutralized, and the graph is in line with higher NO concentrations. There also seems to be something of a reverse poisoning effect, the Al₂O₃-based catalysts are most effective directly after the NO_x pulse than five minutes later, especially visible with the higher NO₂ ratios.



Graph 13: CH₄, CO₂ and NO_x concentrations over Pd/ZSM-5 catalyst at 300°C, for 100% (red), 75% (blue), 50% (green), 25% (pink) and 0% (black) NO in the NO_x gas flow.

The Pd/ZSM-5 catalyst is clearly affected by the NO_x, with decreased efficiency (and increased CH₄ concentration in the outlet gas) as the NO_x gas flow continues. When the NO_x flow is cut of, it requires some time for the CH₄ oxidation to get back to up to speed again. There is a visible accumulation of NO_x that is released once the pulse is ended. It would seem that this release of NO_x corresponds moderately closely to the decrease of CH₄ in the outlet gas, and thus an increase in the reaction rate.

5. Conclusions

The goal of this project was to explore catalysts formulations that would be able to oxidize CH₄ and reduce NO_x at the same time.

Of the catalysts tested, the Pd/In/Al₂O₃ catalyst seems to be the most promising, with the Pd/In/ZSM-5 being the least promising and the two without indium is of intermediate interest. Pd/In/Al₂O₃ has a higher, or at least equal reaction rate for CH₄ at all temperatures compared to the other catalysts, and also seems to be less affected by the NO_x. However, there was only a relatively small reduction of NO_x for all catalysts.

The results achieved in the first experiment, specifically the delay when heating the catalysts again, might be due to hysteresis. This means that the reaction requires additional energy to

overcome the energy barrier, but once overcome, it can continue even with less energy. However, after extinction, an additional boost in energy is required to start it up again.

It would also seem that the Indium has some influence over CH₄ oxidation and NO oxidation to NO₂, but doesn't seem to affect the NO_x breakdown to free N and O.

The different supports, ZSM-5 and Al₂O₃, differs in accumulation of NO_x, with ZSM-5 accumulating more at higher temperatures, and less at lower temperatures, compared to Al₂O₃. It also seems to be more sensitive to NO_x poisoning, especially at higher temperatures, though this might be because of the higher amount of accumulated NO_x.

6. Future Work

It would be useful to further study the catalysts produced. At present, there is no knowledge about things like their total surface area or the distribution of the catalytic particles, things that would perhaps go further in explaining some of the behaviors shown.

The Pd/In/ZSM-5 catalyst showed a result much lower than expected. It was chosen in an attempt to design the optimal catalyst, but showed the lowest conversions of all four, while Pd/In/Al₂O₃ showed the best. Therefore, it would perhaps be beneficial to examine this catalyst and try to determine what is preventing it from performing as expected. A possible explanation could be a lower than expected or uneven Indium application. Another possibility is that the interaction between the In, Pd and/or ZSM-5 base creates some unexpected difficulties.

Further, it would be beneficial to investigate if there are any other products from the methane. Only CO₂ were found in any significant quantities, but in the first experiment, it would seem that not all carbon is accounted for between the CO₂ and CH₄ at high temperatures.

Finally, it would be interesting to study the NO_x poisoning closer, in part to study the exact mechanisms of it, and also to try to find ways to prevent it. At the same time, it would be interesting to investigate the moderately large "hump" in NO_x concentration that appeared in the first experiment when the catalysts were heated again.

7. Acknowledgements

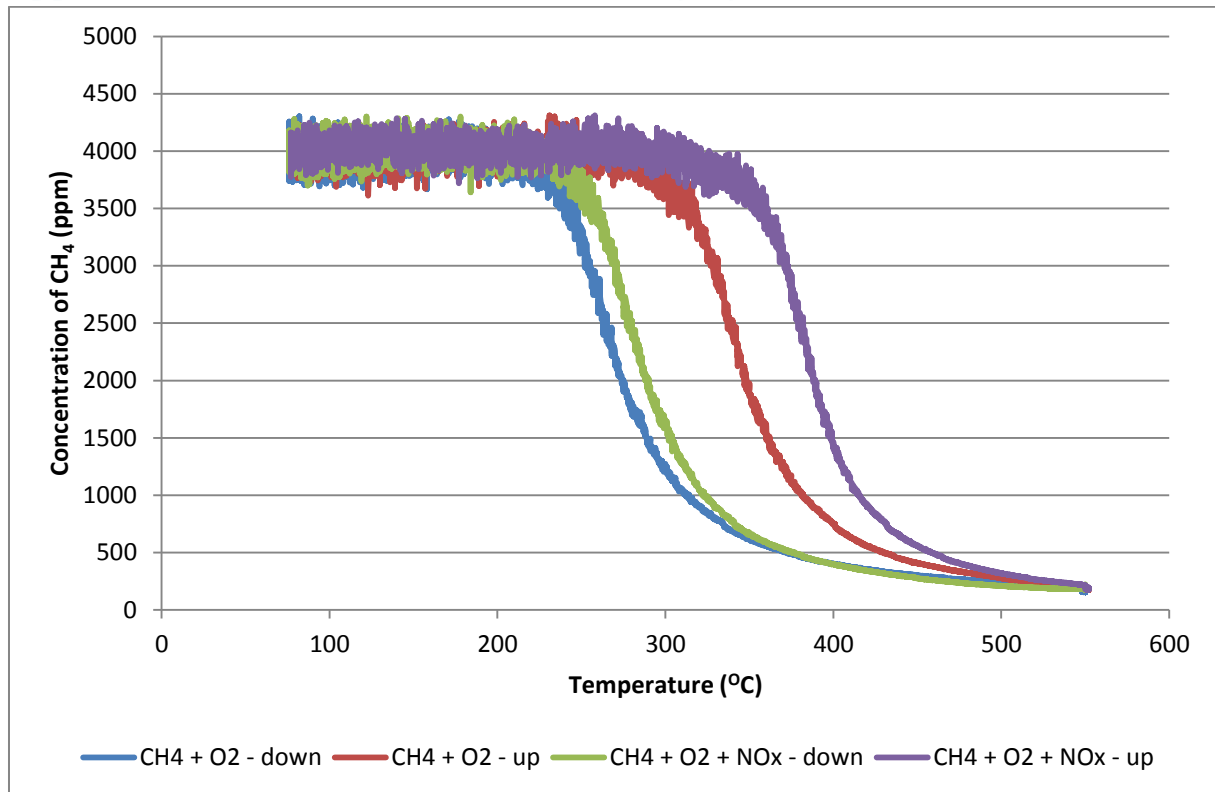
A big thank you to Hanna Härelind, my examiner, and Per-Anders Carlsson, my supervisor, for giving me the opportunity to do this master thesis project, and for being supportive when things didn't always go exactly as planned.

I would also like to thank Fredrik Gunnarsson for explaining, showing and helping me with the sol-gel method of catalyst preparation and Marika Männikkö for demonstrating the experimental flow reactor setup and the FTIR apparatus.

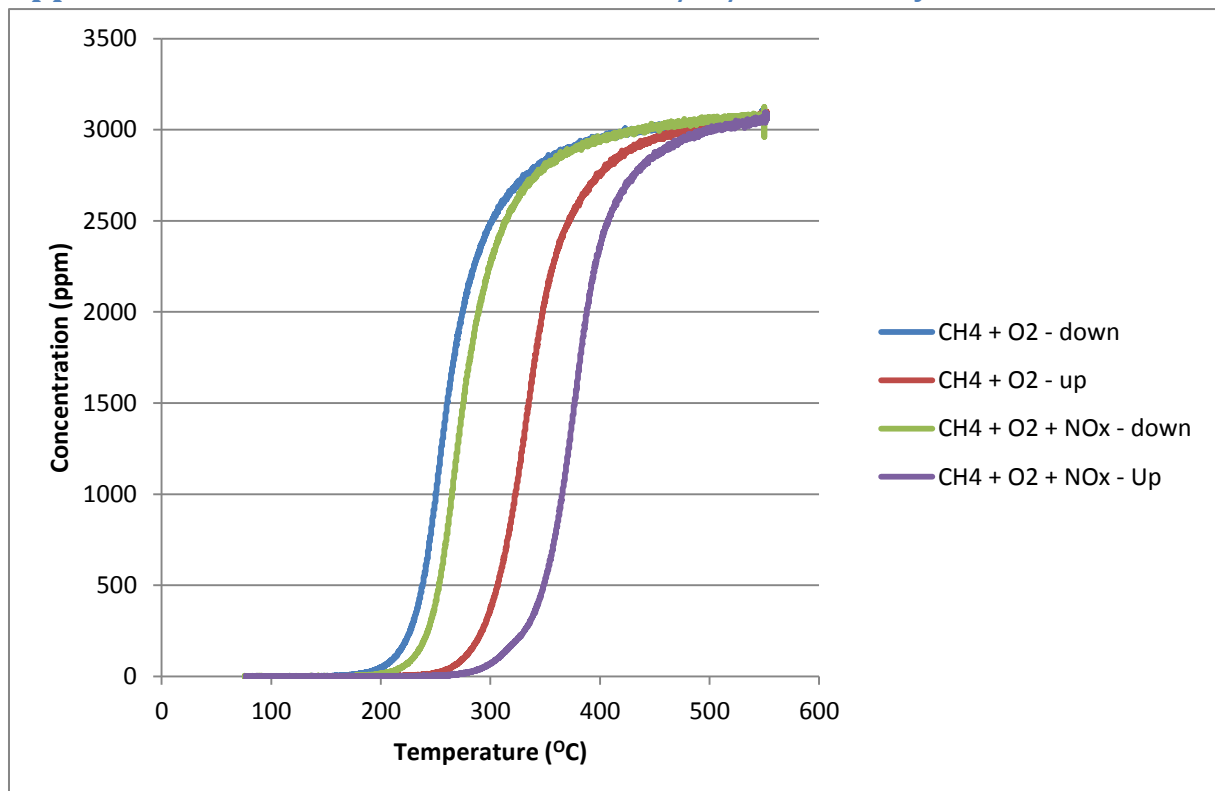
And, of course, thank you to mom and dad, always supportive, and my friends.

Appendix A: Gas concentration graphs for evaluation experiment

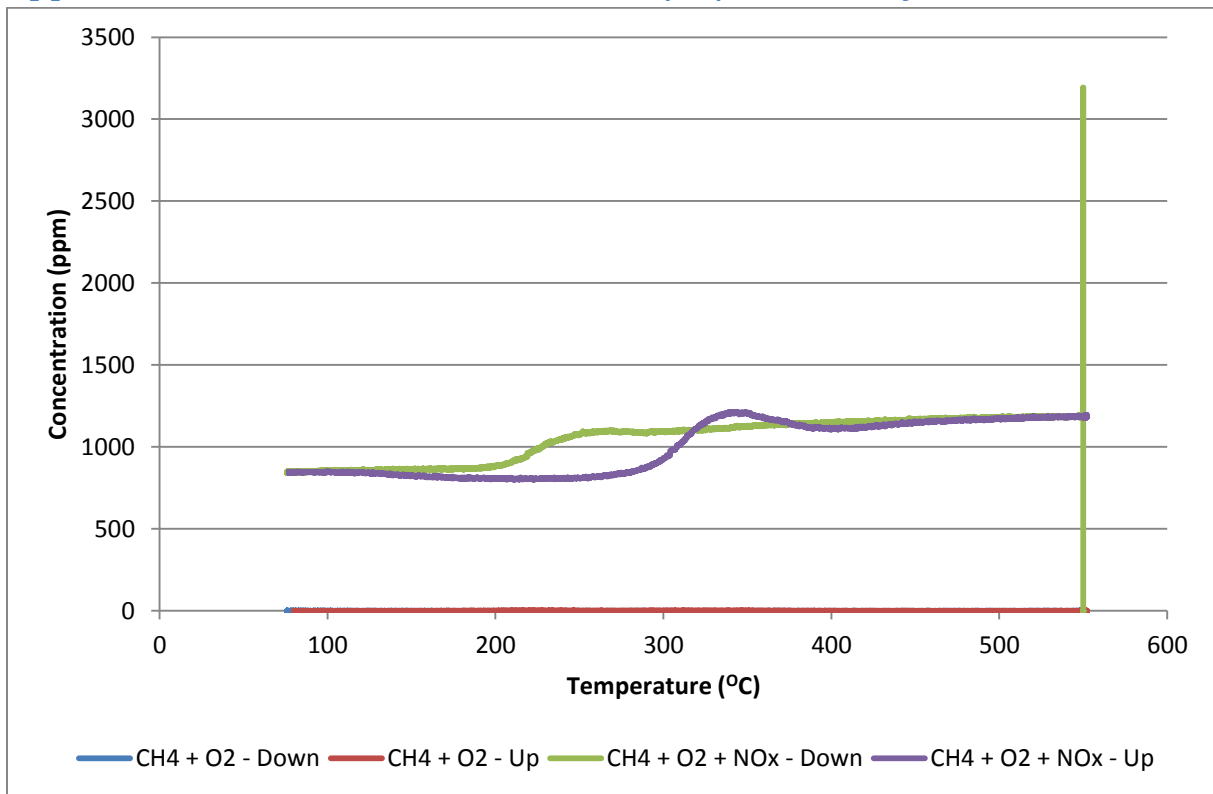
Appendix A1.1: CH₄ concentration over Pd/In/Al₂O₃ catalyst



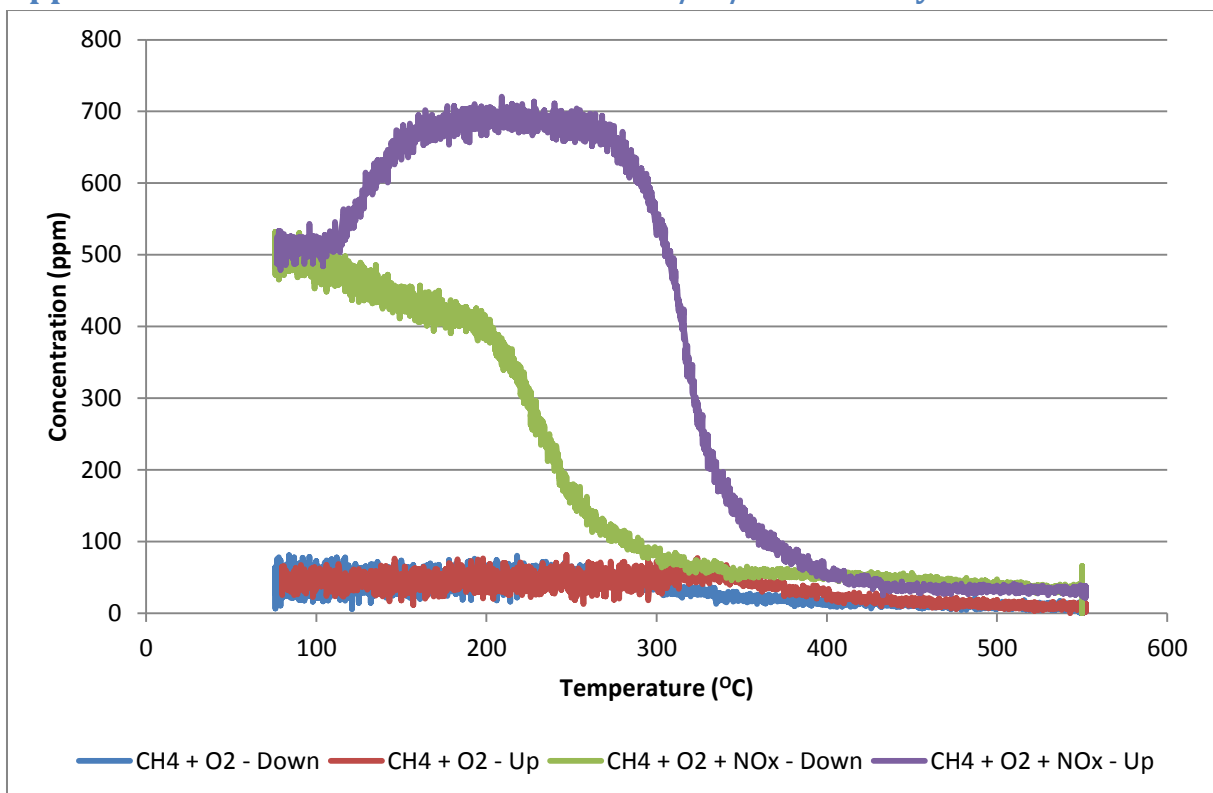
Appendix A1.2: CO₂ concentration over Pd/In/Al₂O₃ catalyst



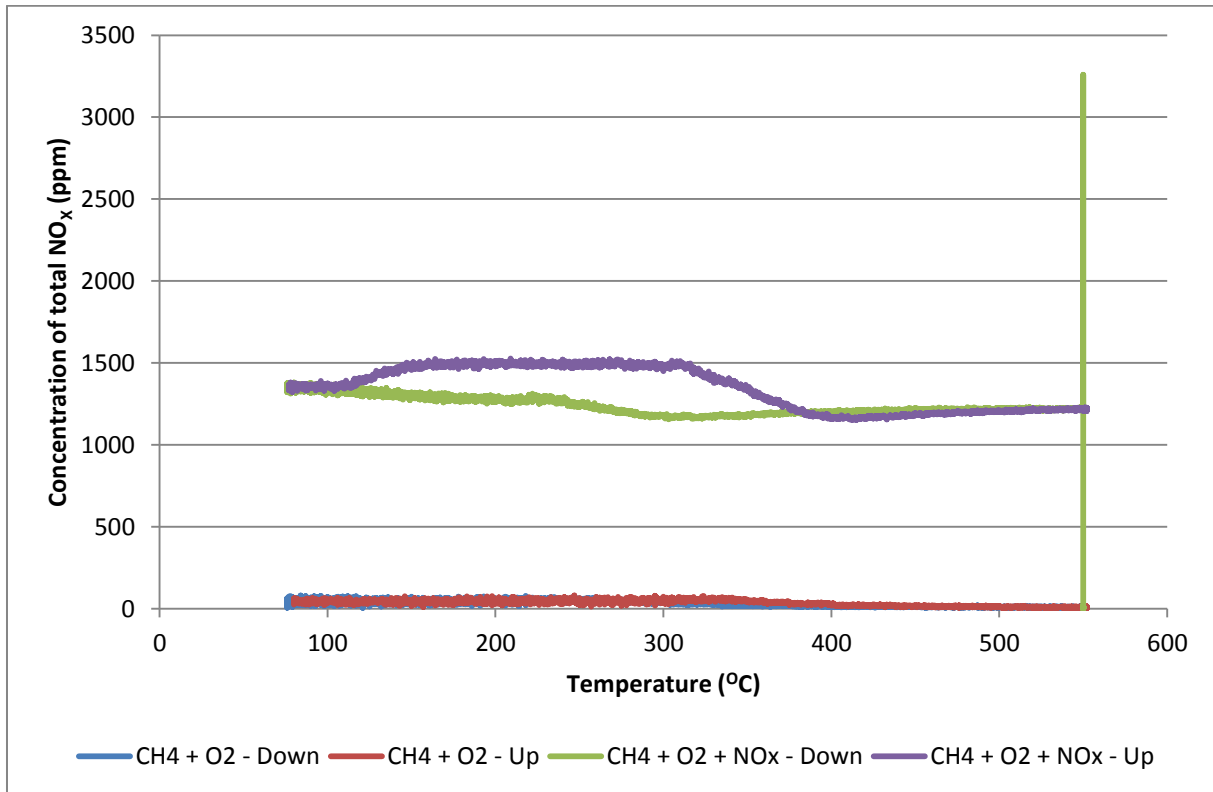
Appendix A1.3: NO concentration over Pd/In/Al₂O₃ catalyst



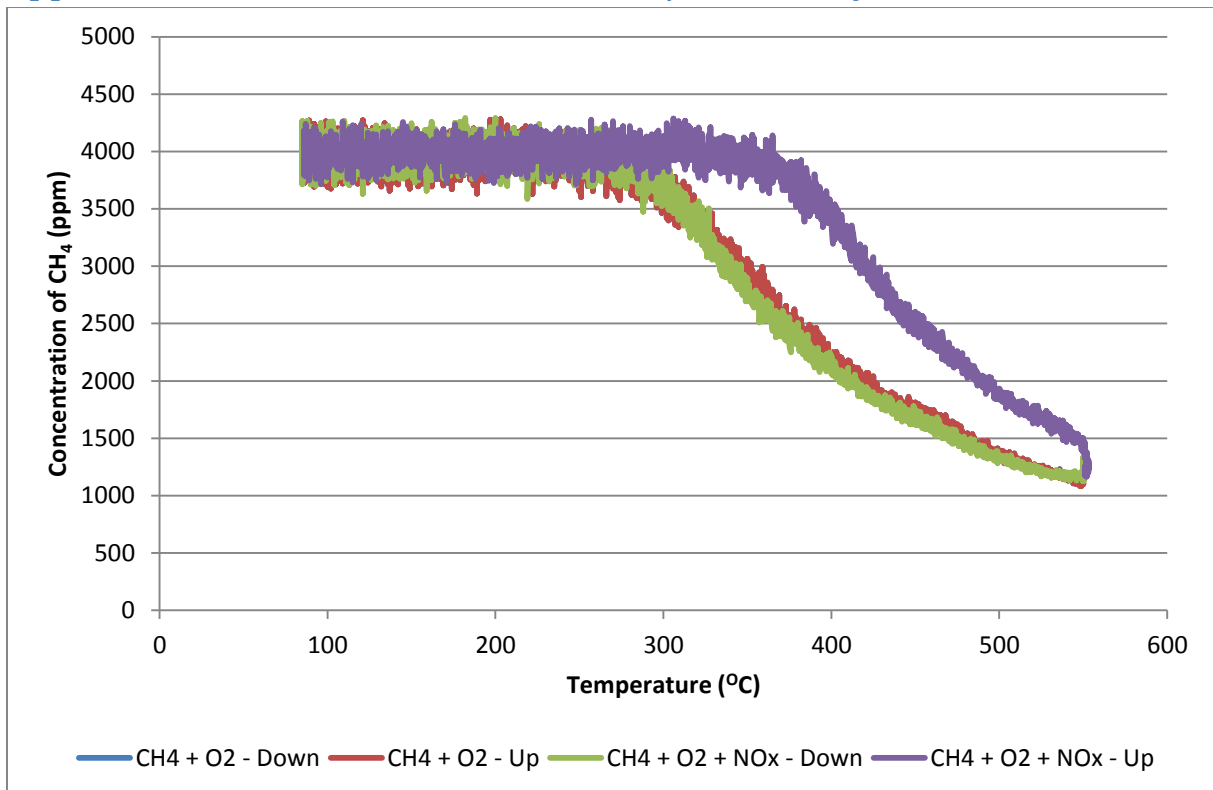
Appendix A1.4: NO₂ concentration over Pd/In/Al₂O₃ catalyst



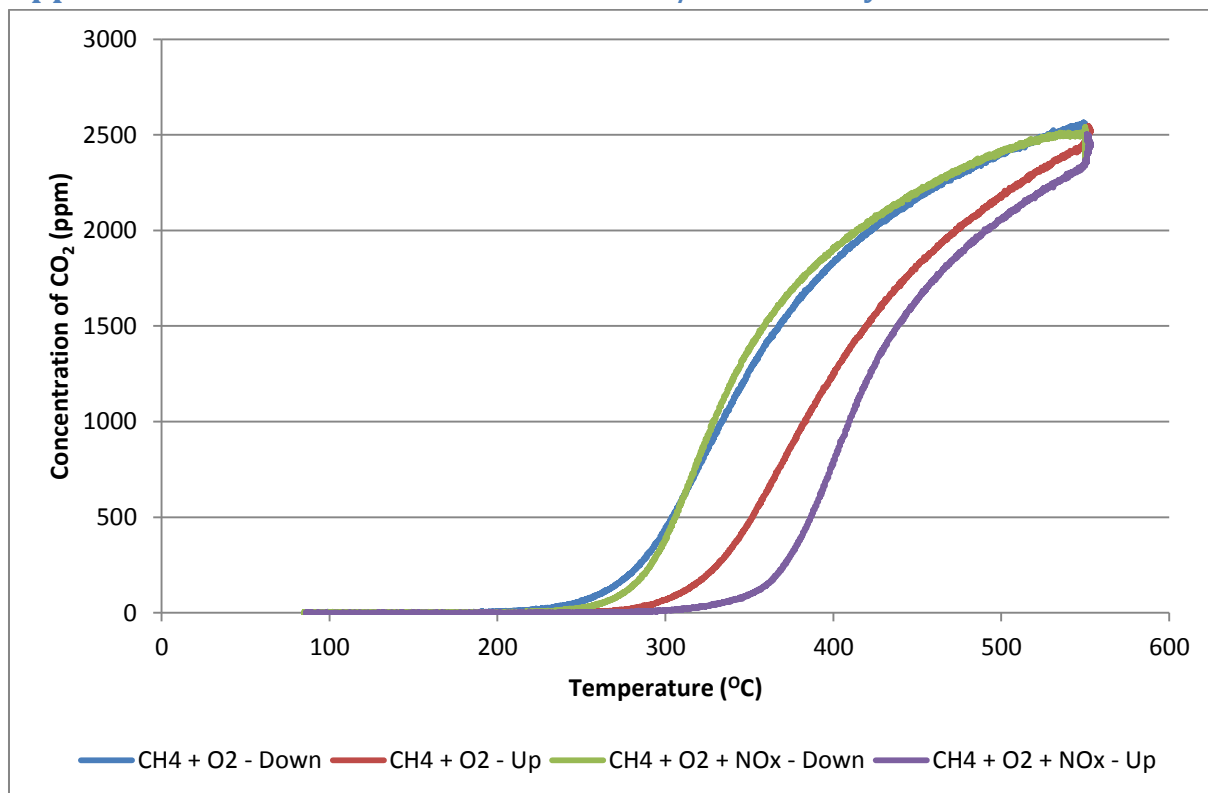
Appendix A1.5: Total NO_x concentration over Pd/In/Al₂O₃ catalyst



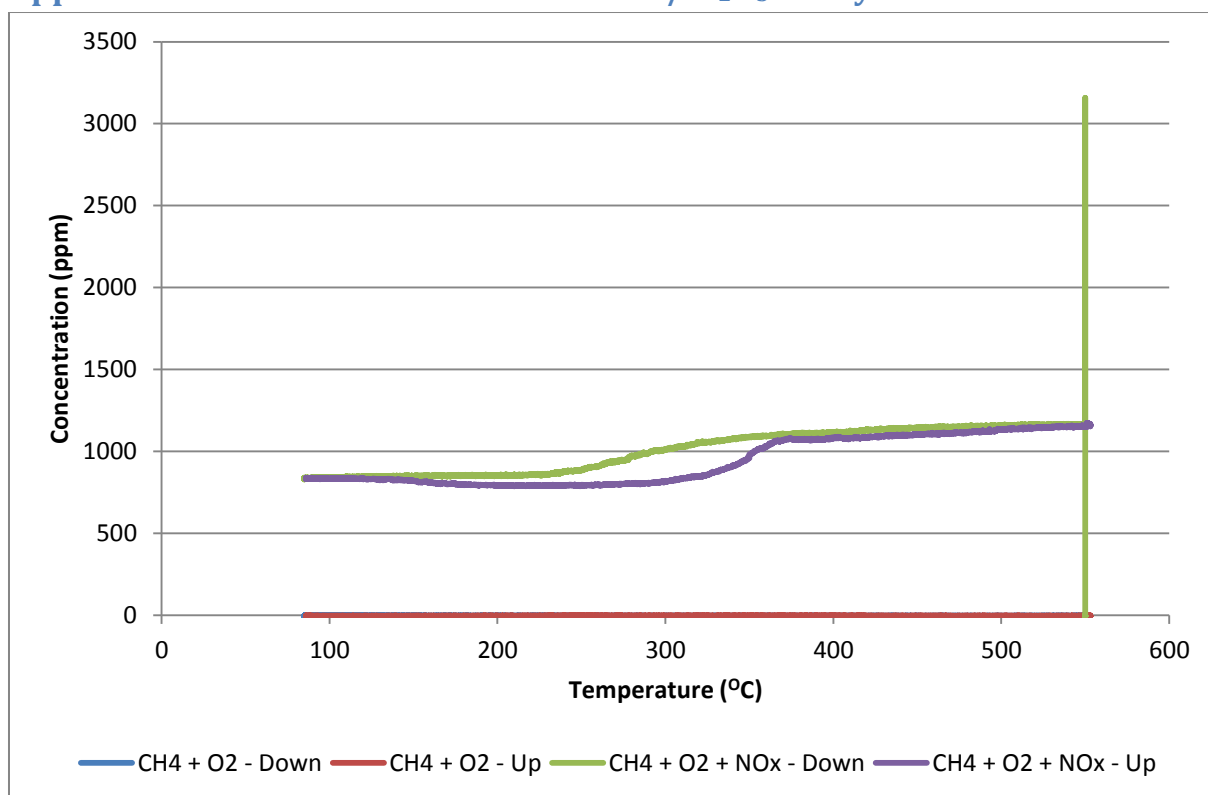
Appendix A2.1 CH₄ concentration over Pd/Al₂O₃ catalyst



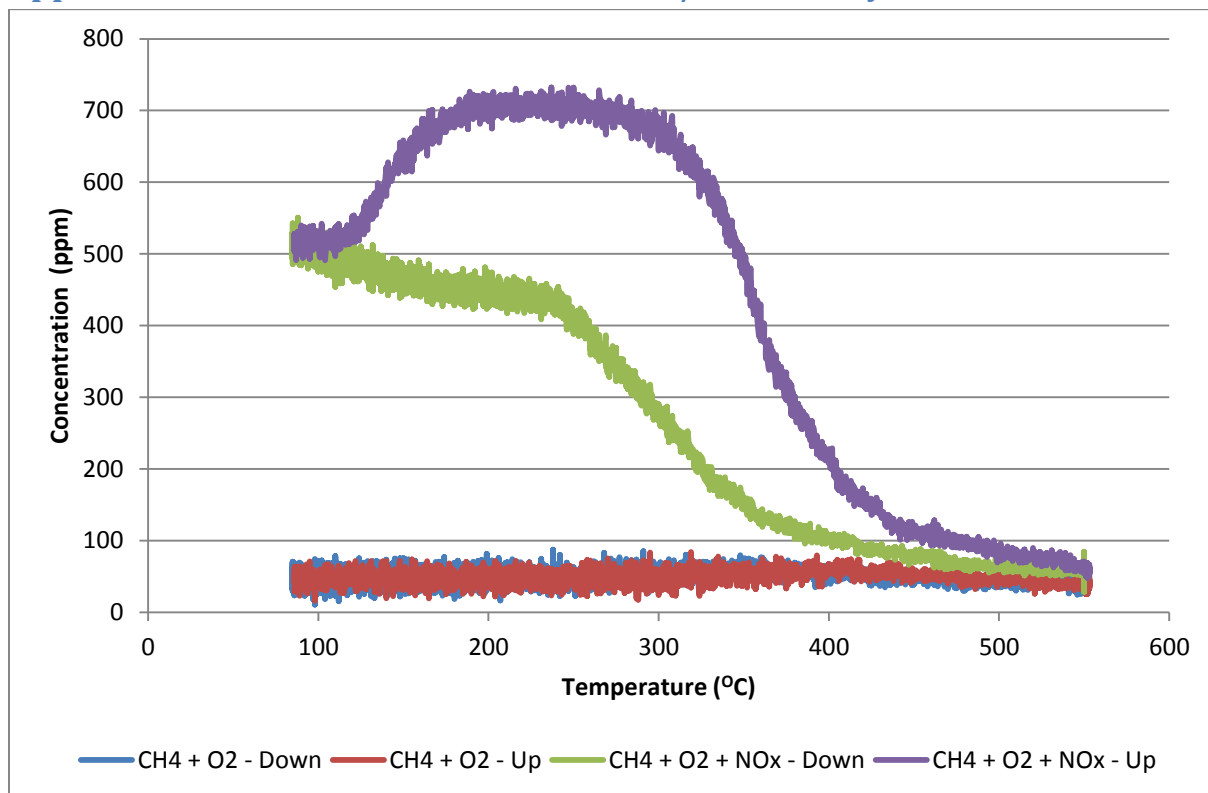
Appendix A2.2: CO₂ concentration over Pd/Al₂O₃ catalyst



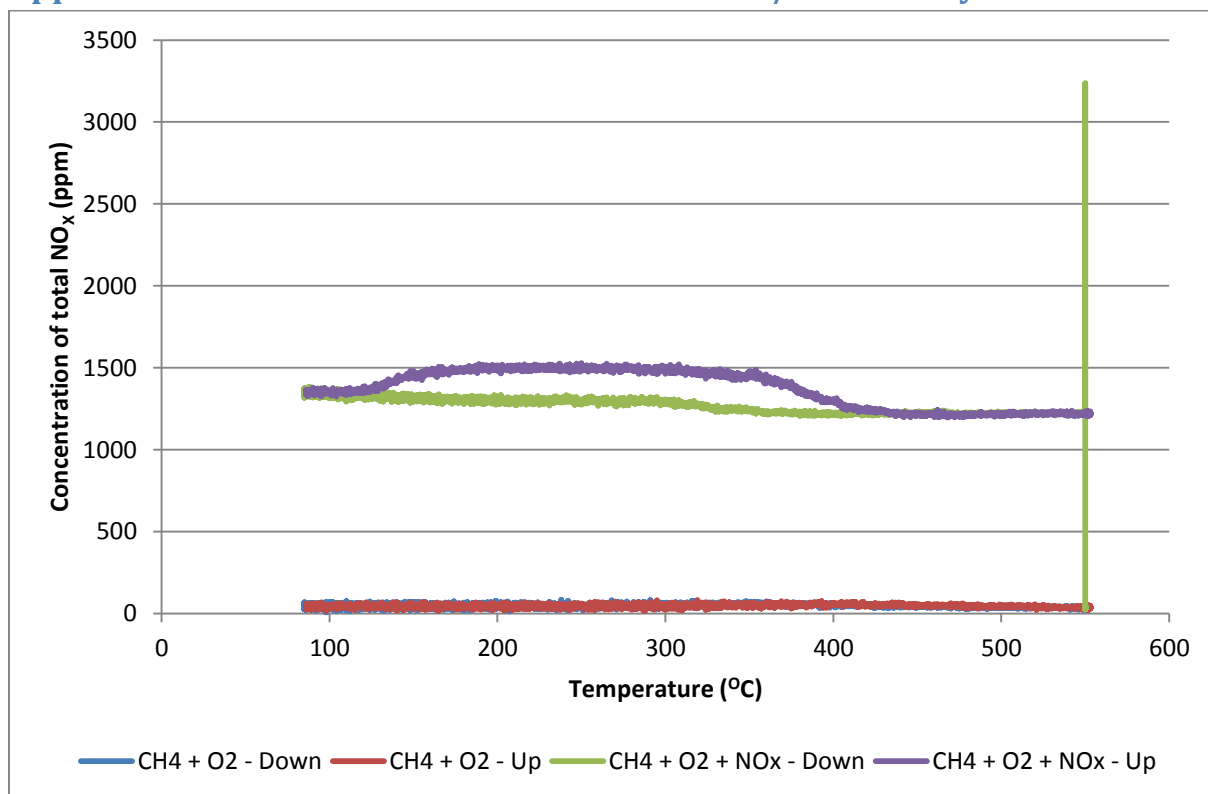
Appendix A2.3: NO concentration over Pd/Al₂O₃ catalyst



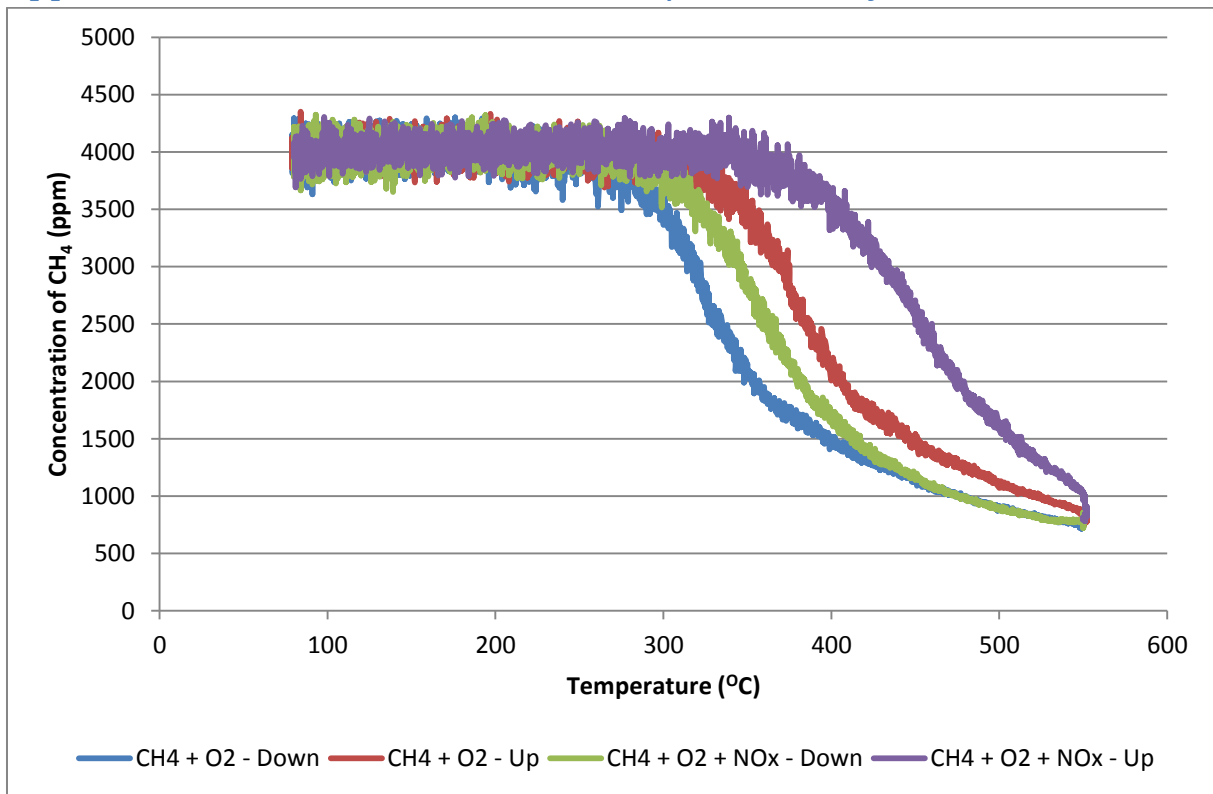
Appendix A2.4: NO₂ concentration over Pd/Al₂O₃ catalyst



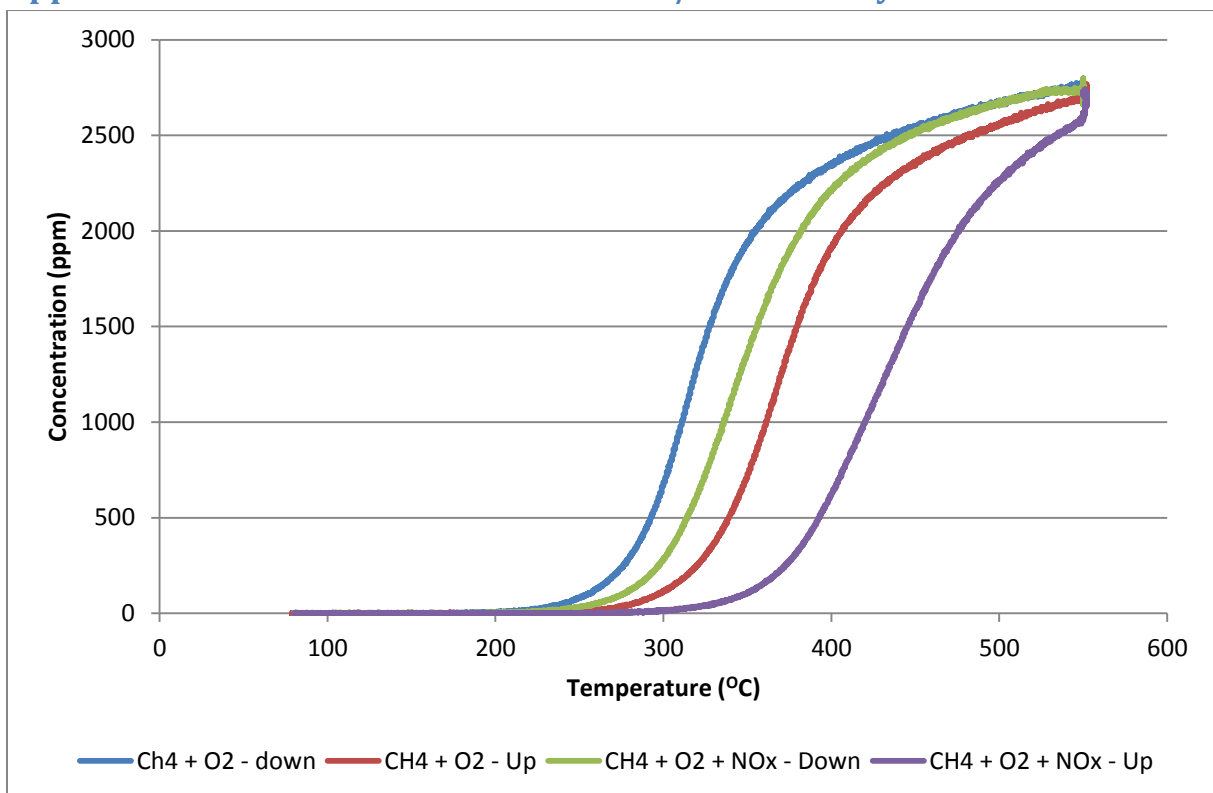
Appendix A2.5: Total NO_x concentration over Pd/Al₂O₃ catalyst



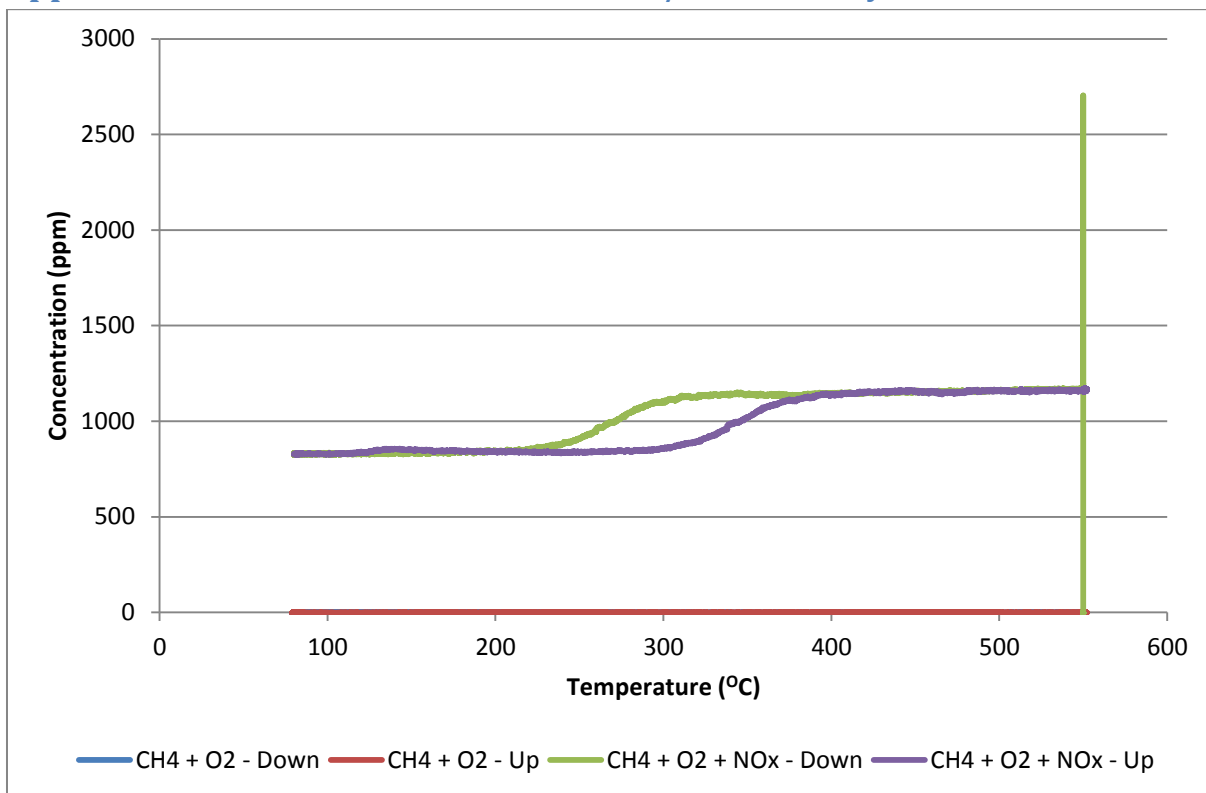
Appendix A3.1 CH₄ concentration over Pd/ZSM-5 catalyst



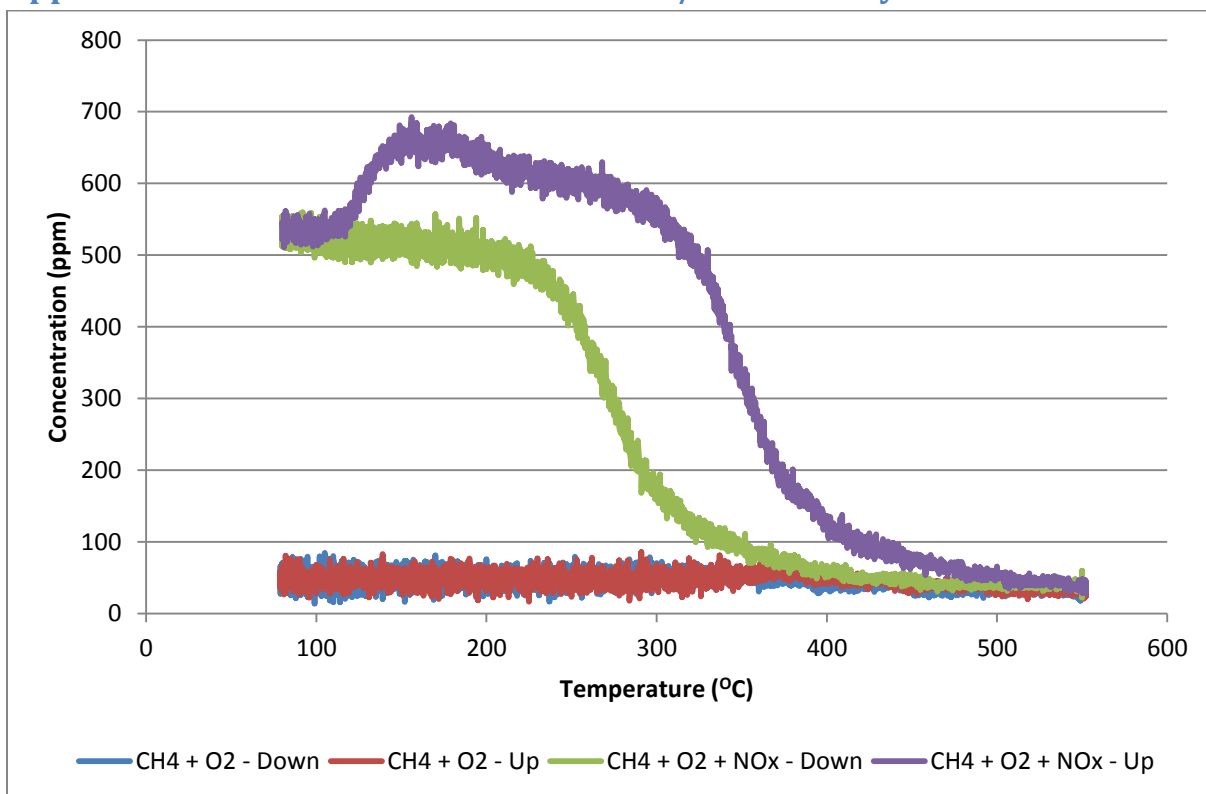
Appendix A3.2: CO₂ concentration over Pd/ZSM-5 catalyst



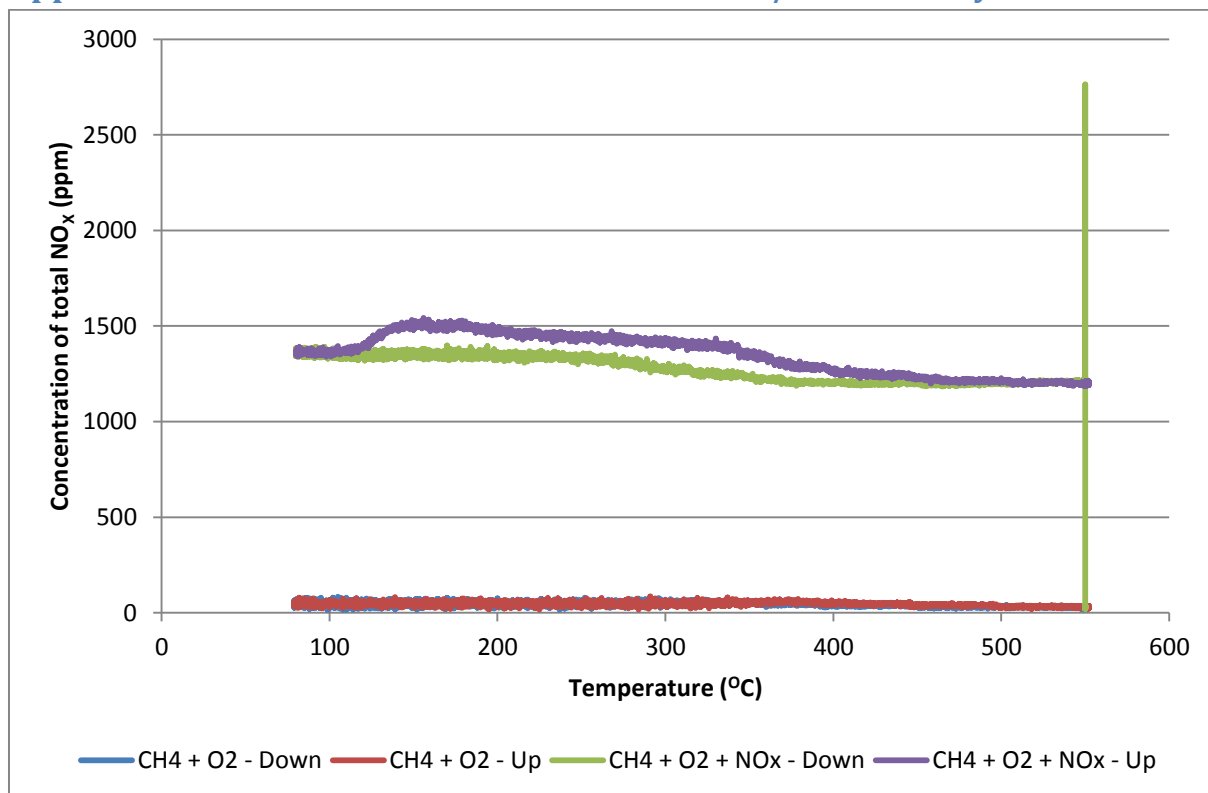
Appendix A3.3: NO concentration over Pd/ZSM-5 catalyst



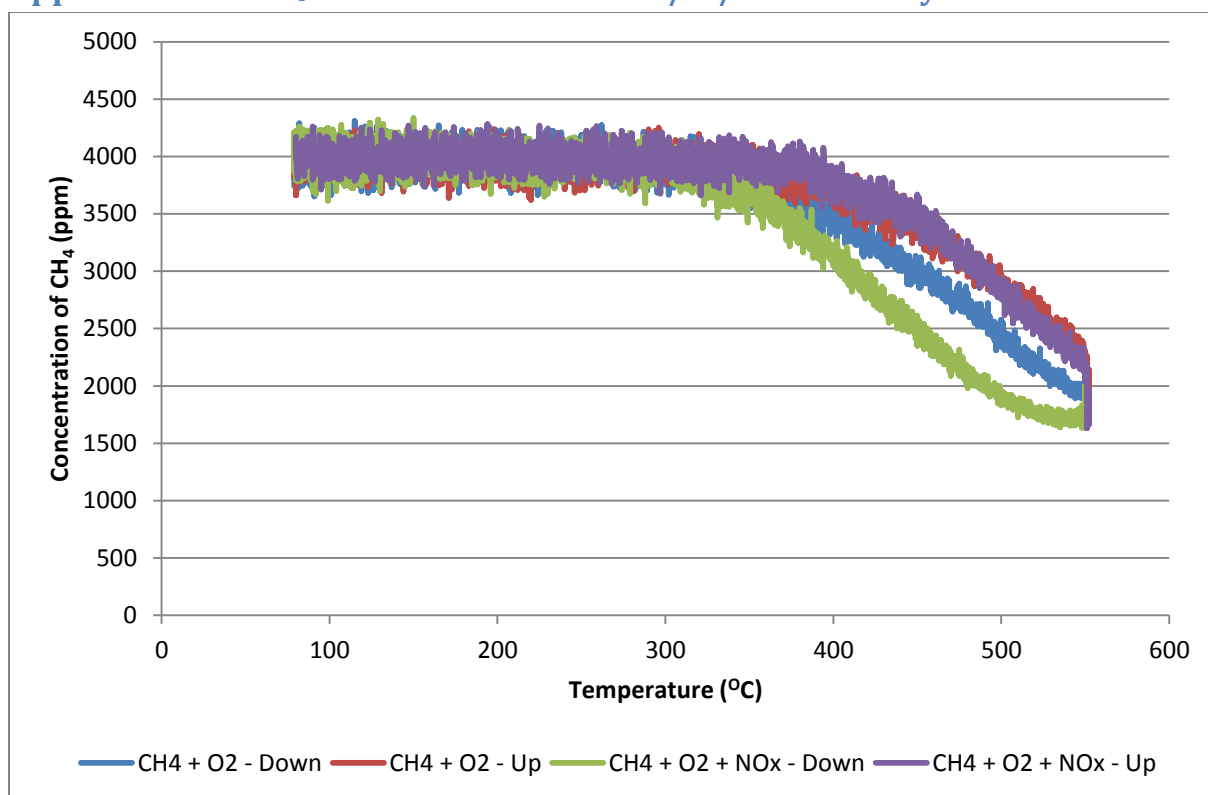
Appendix A3.4: NO₂ concentration over Pd/ZSM-5 catalyst



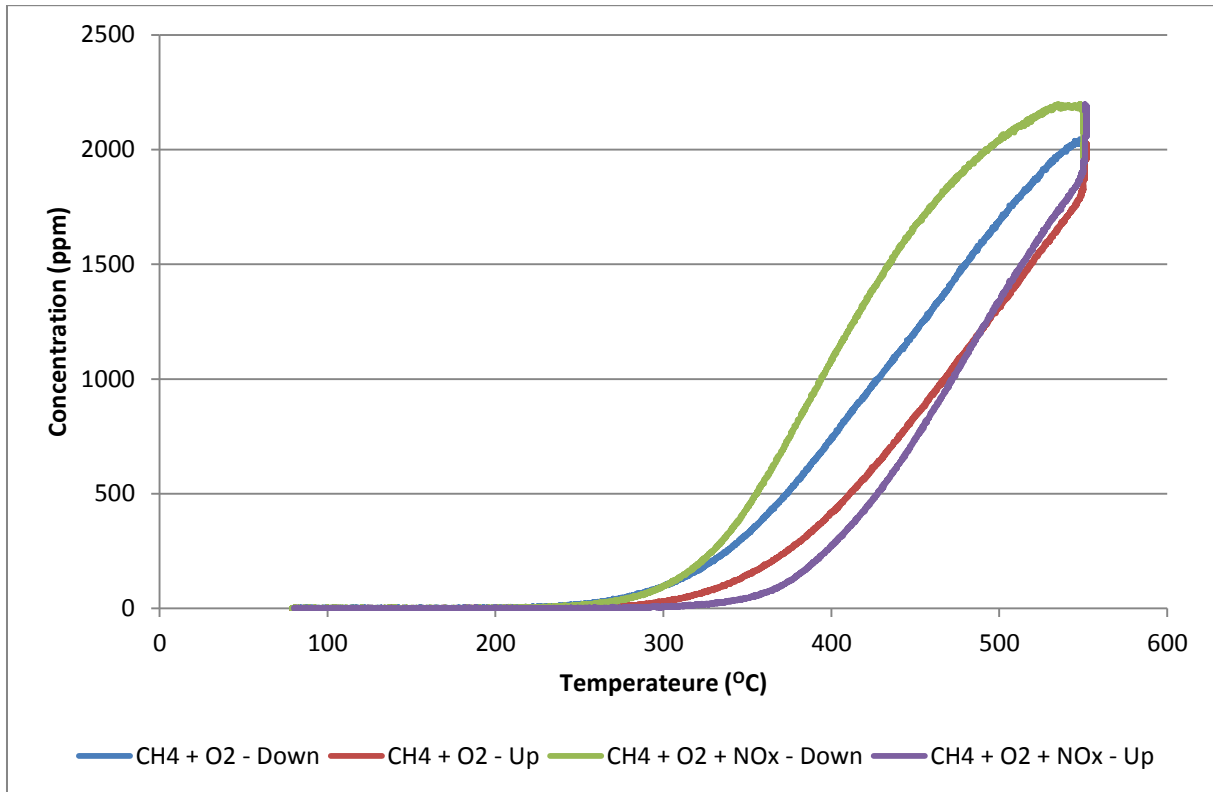
Appendix A3.5: Total NO_x concentration over Pd/ZSM-5 catalyst



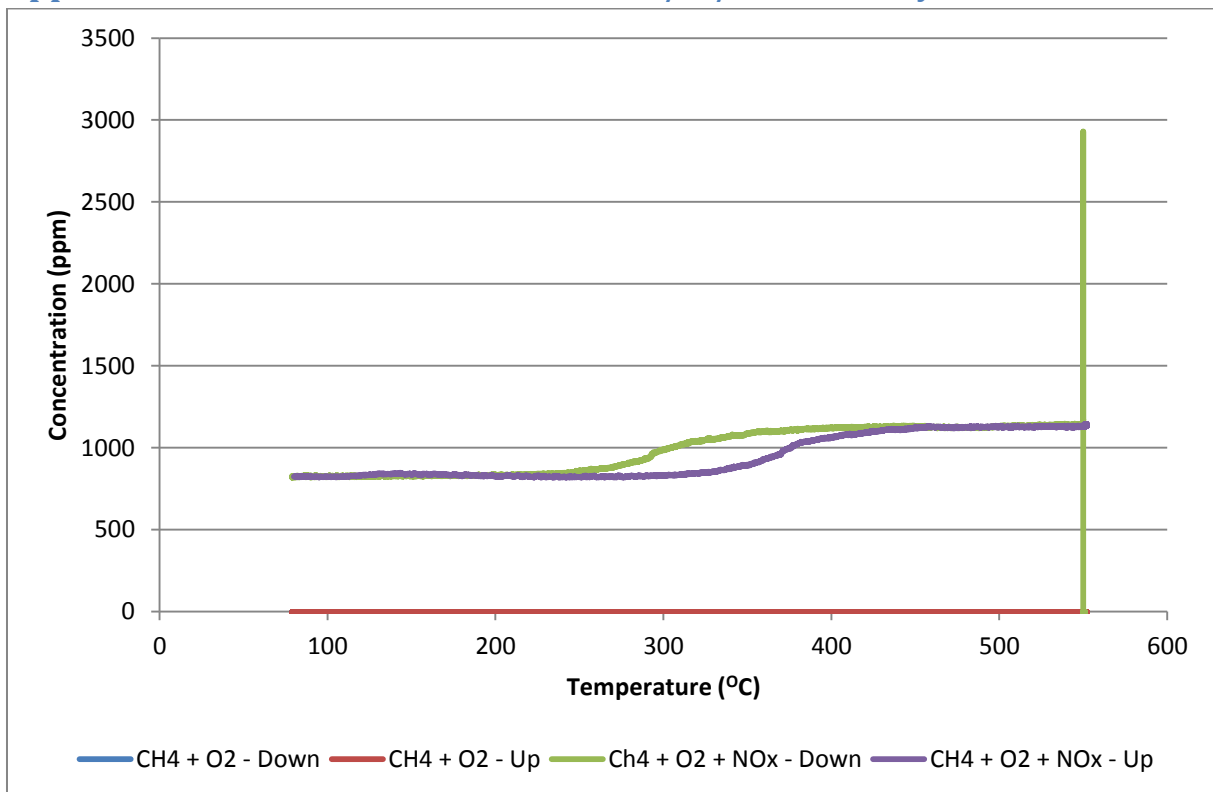
Appendix A4.1 CH₄ concentration over Pd/In/ZSM-5 catalyst



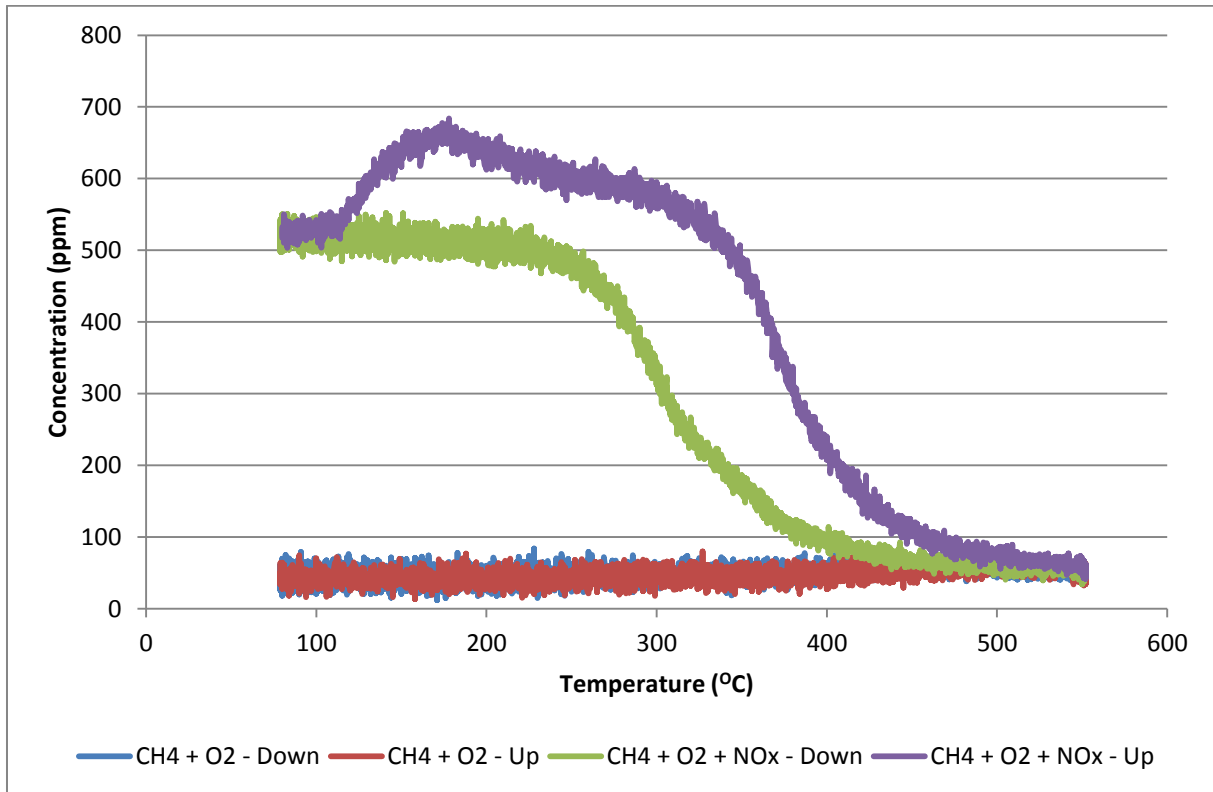
Appendix A4.2: CO₂ concentration over Pd/In/ZSM-5 catalyst



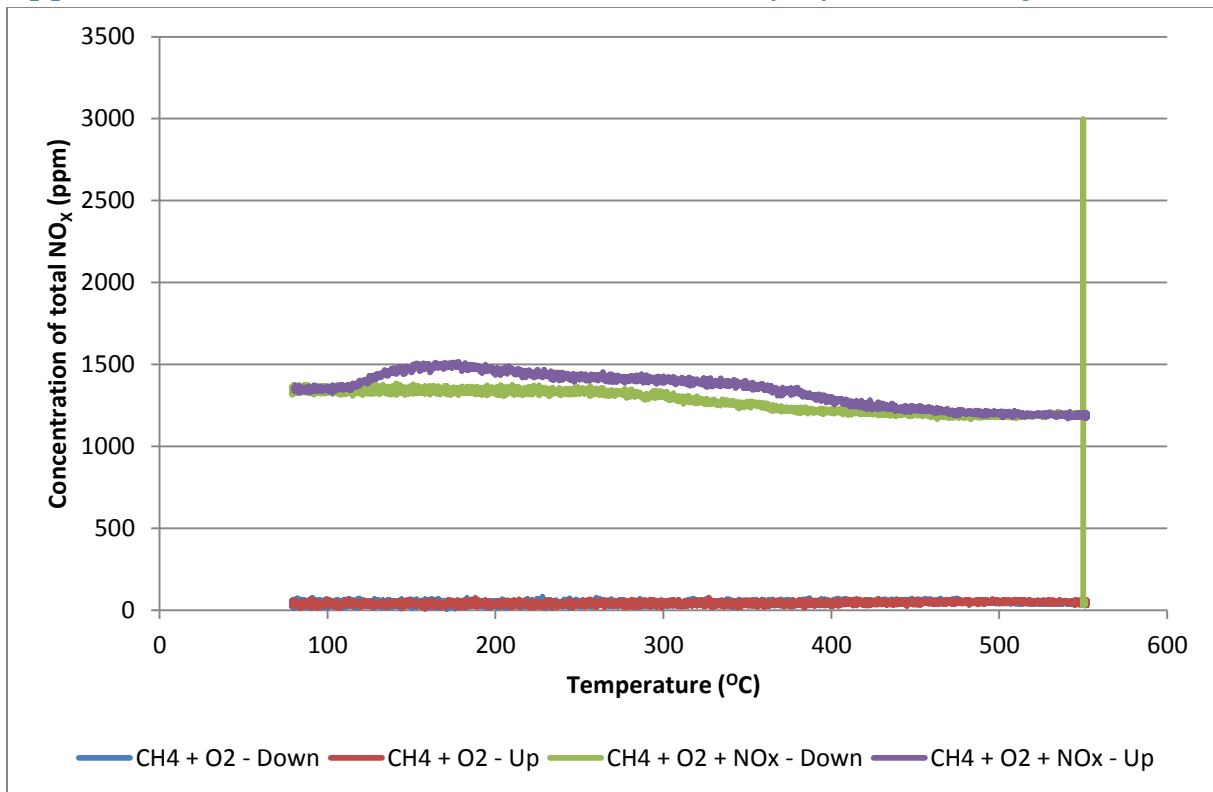
Appendix A4.3: NO concentration over Pd/In/ZSM-5 catalyst



Appendix A4.4: NO₂ concentration over Pd/In/ZSM-5 catalyst

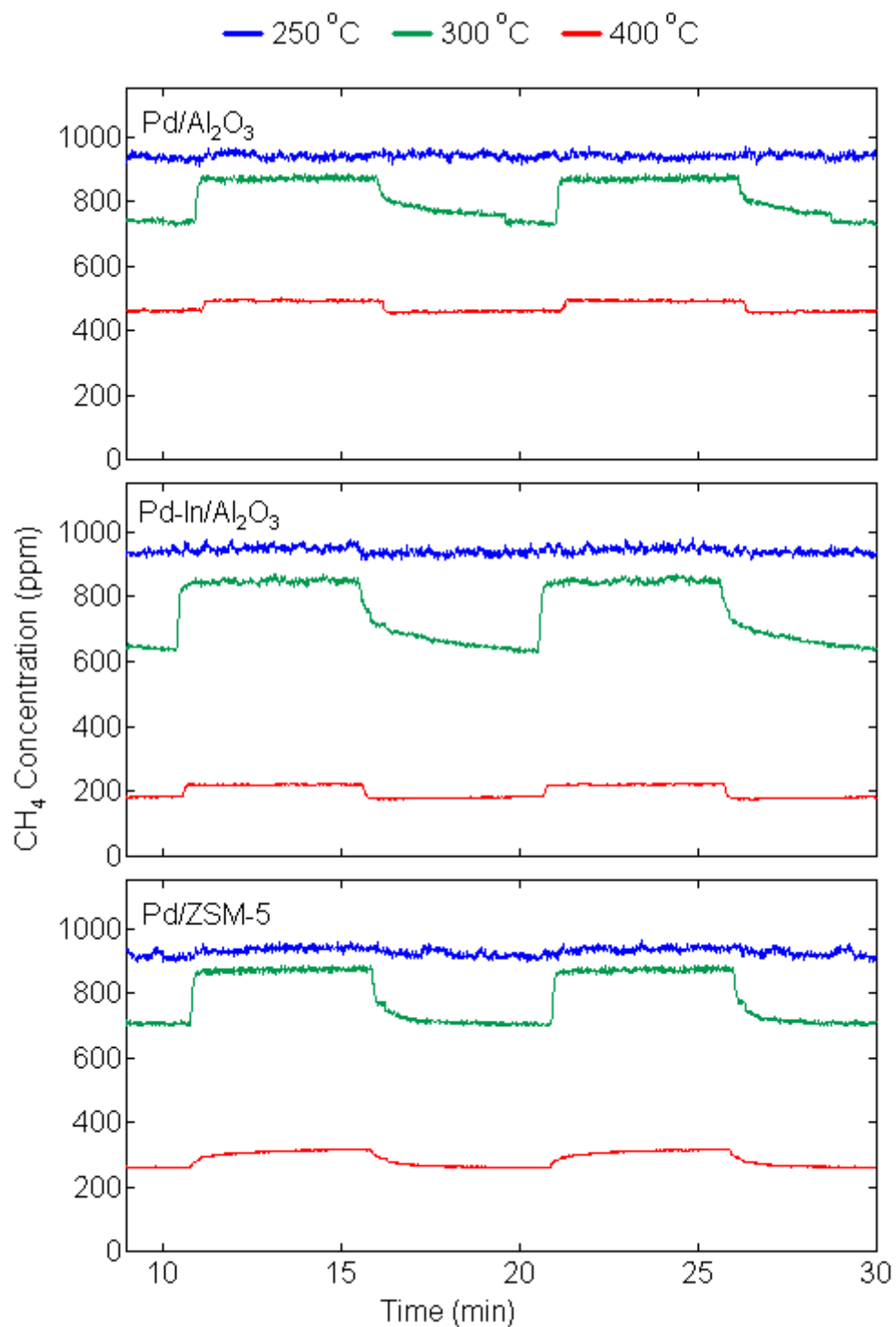


Appendix A4.5: Total NO_x concentration over Pd/In/ZSM-5 catalyst

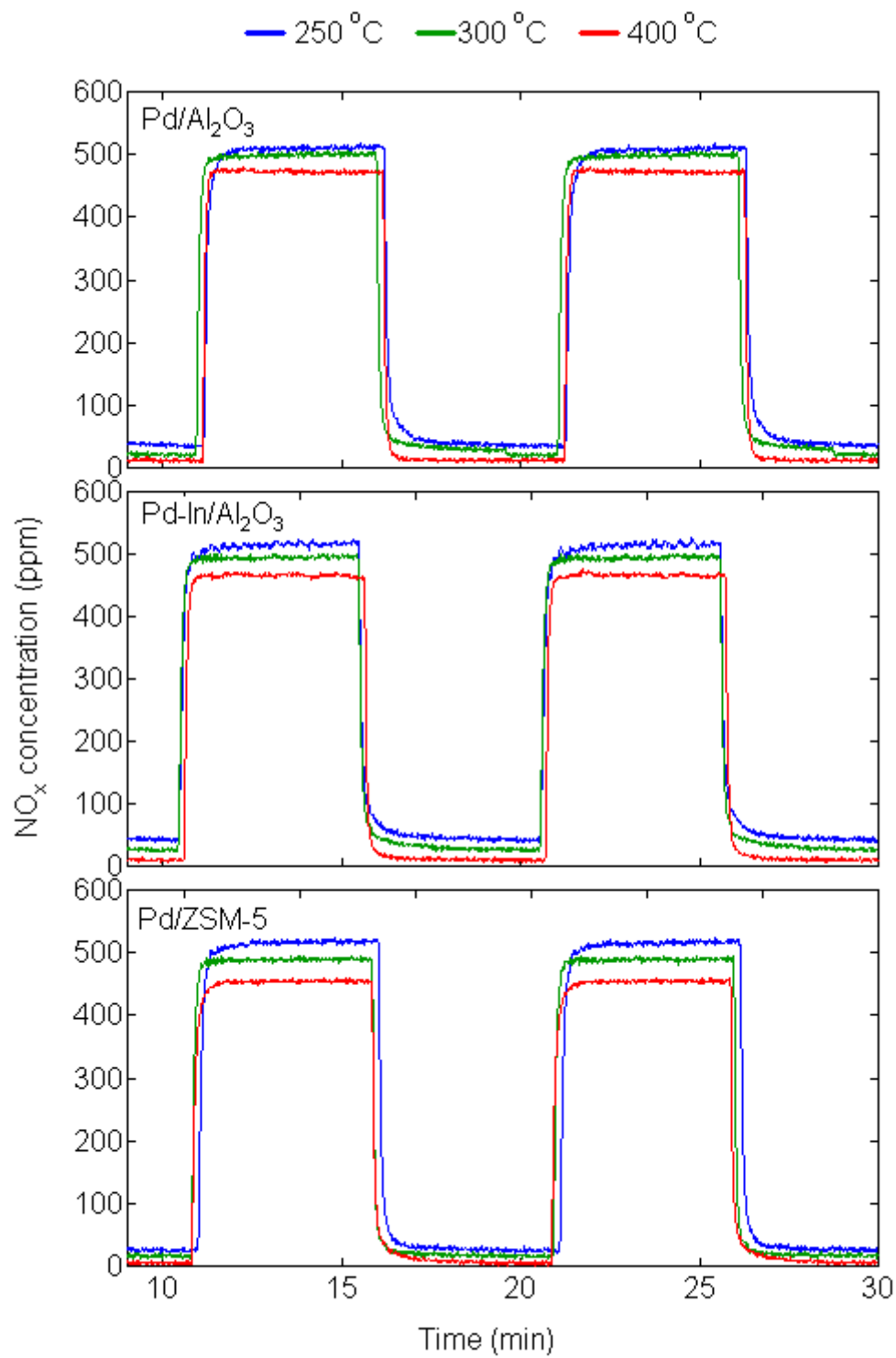


Appendix B: Gas concentration graphs for transient pulse experiment

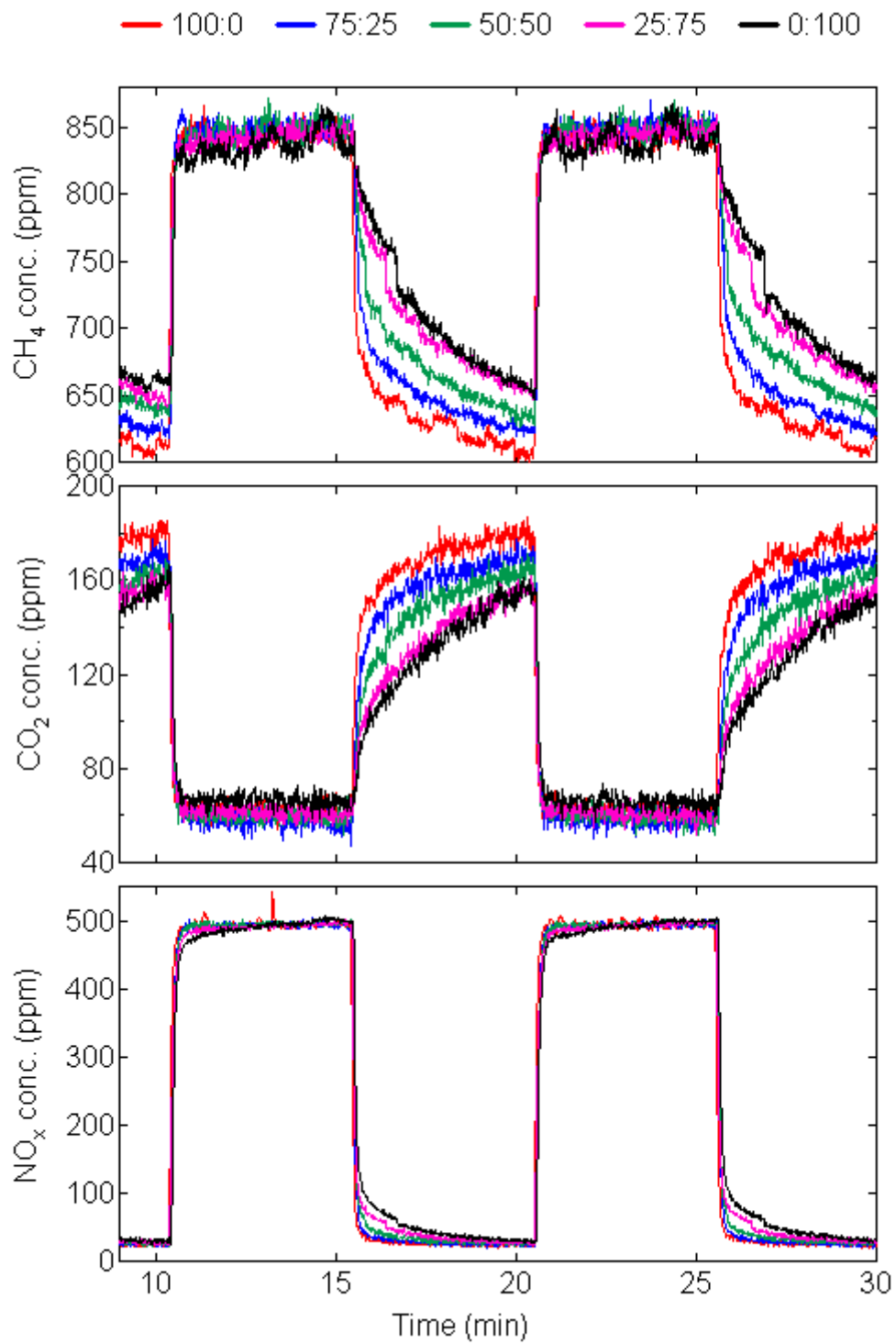
Appendix B1.1: CH₄ gas concentration graphs for 50% NO over all catalysts at all temperatures



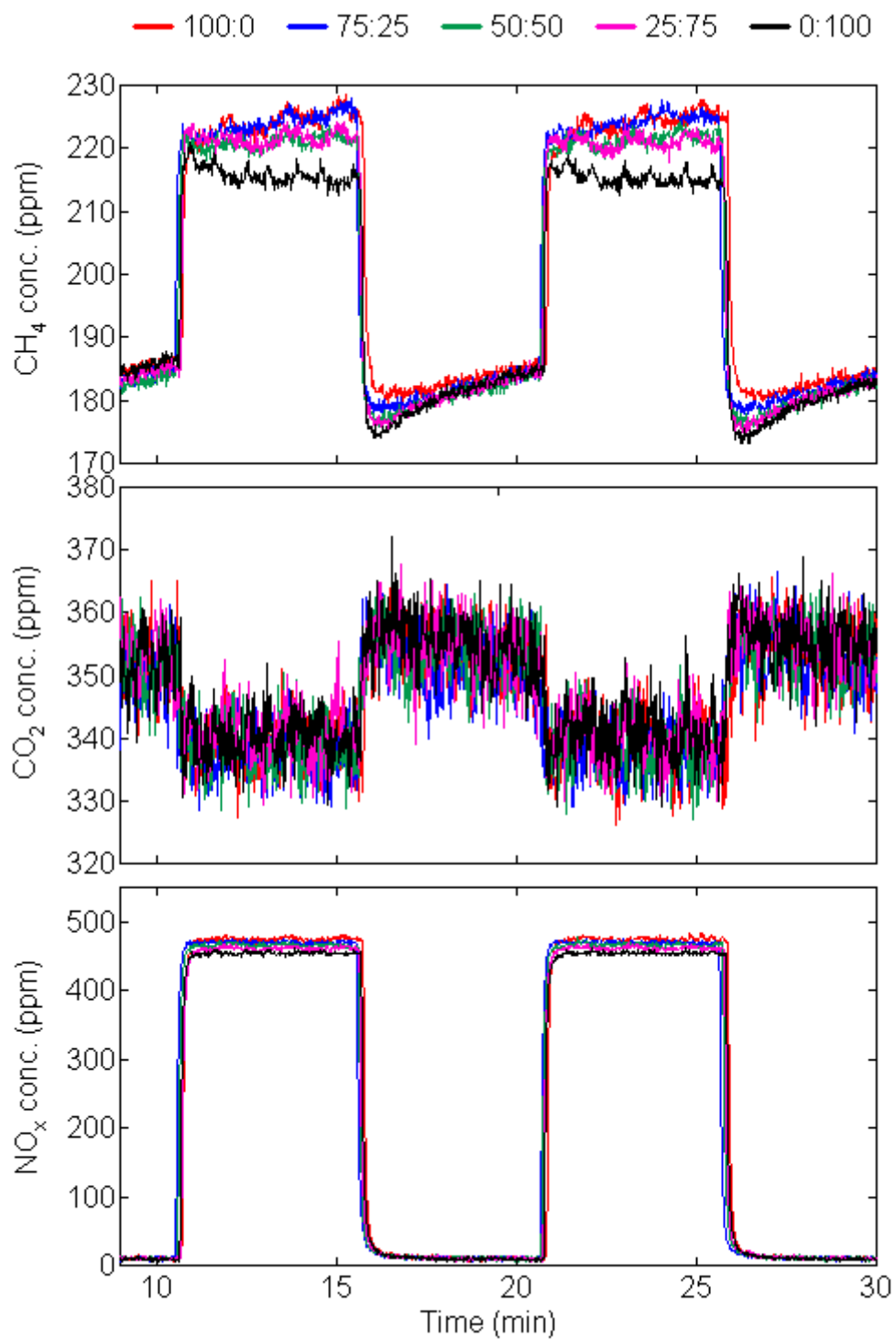
Appendix B1.2: NO_x gas concentration graphs for 50% NO over all catalysts at all temperatures



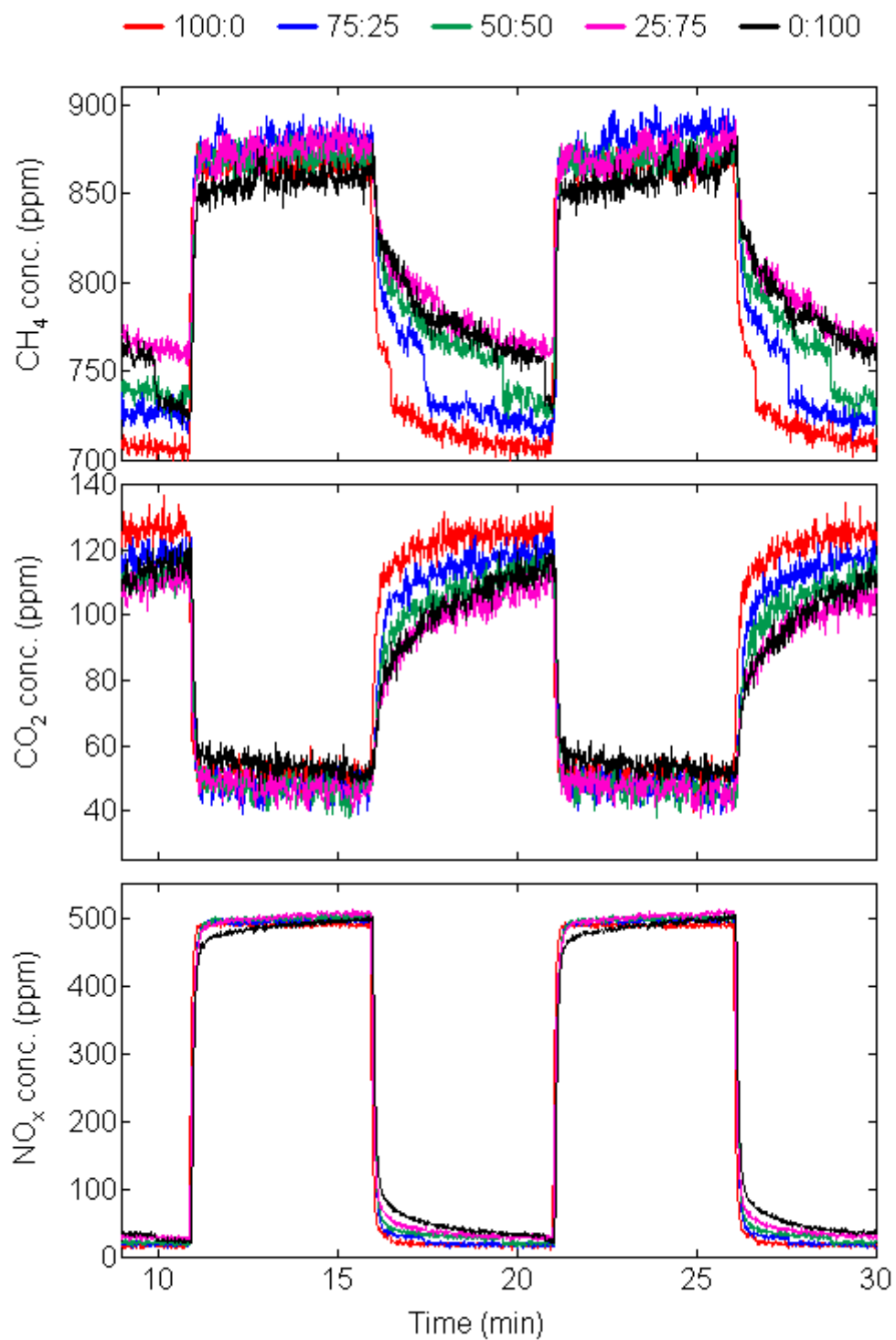
Appendix B2.1: CH₄, CO₂ and NO_x gas concentration graphs for all NO concentration over Pd/In/Al₂O₃ catalyst at 300°C



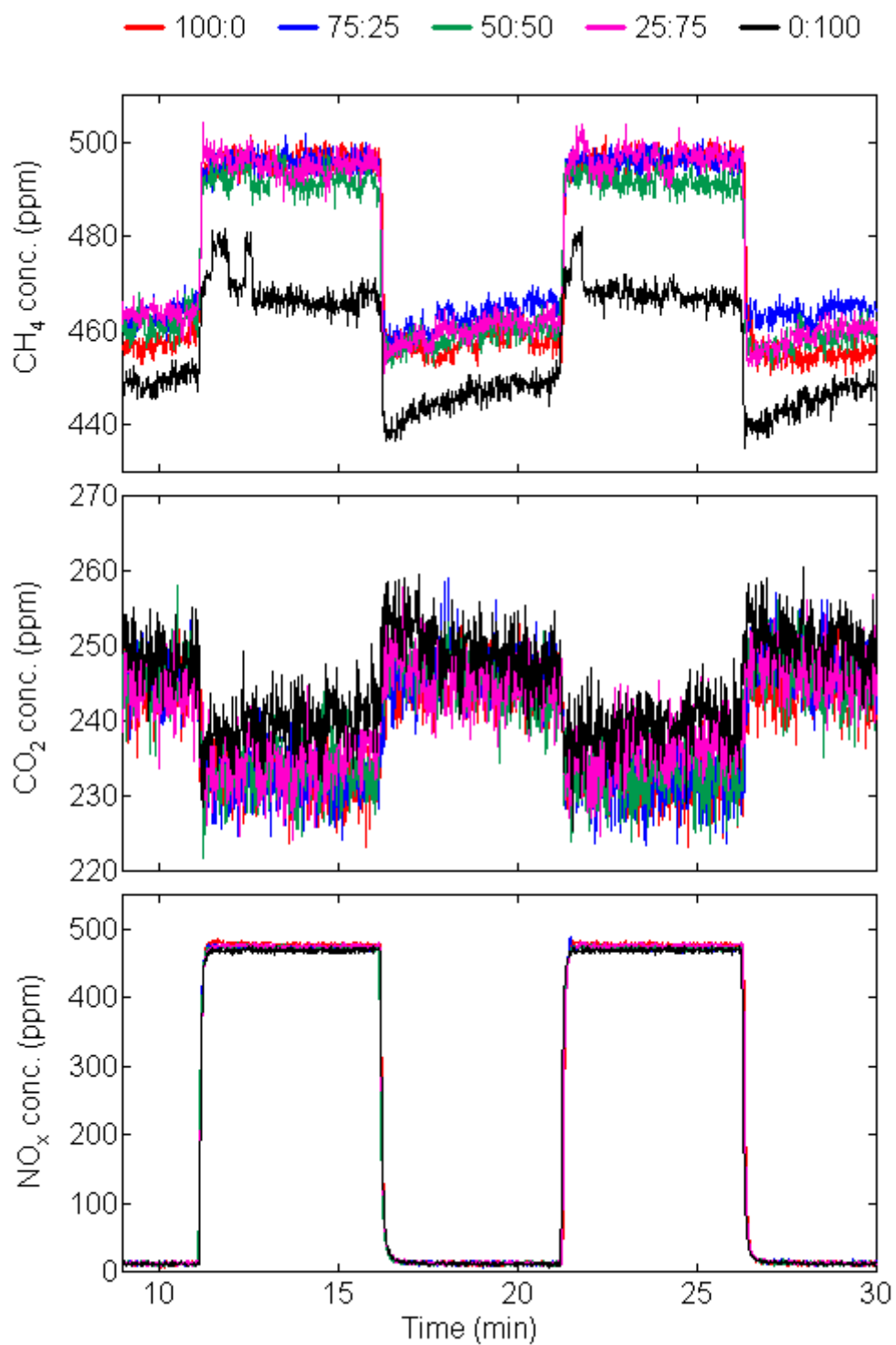
Appendix B2.2: CH₄, CO₂ and NO_x gas concentration graphs for all NO concentration over Pd/In/Al₂O₃ catalyst at 400°C



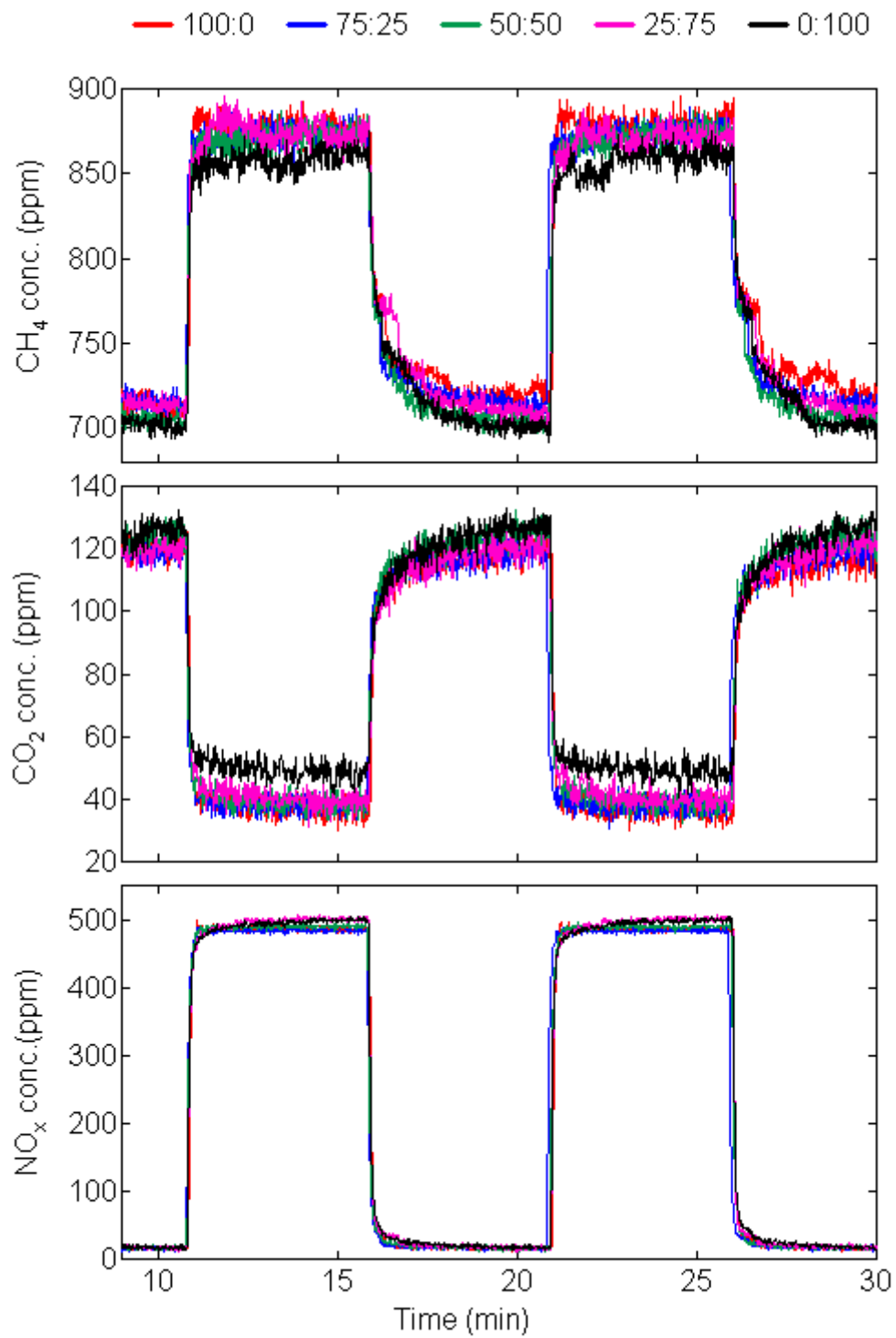
Appendix B3.1: CH₄, CO₂ and NO_x gas concentration graphs for all NO concentration over Pd/Al₂O₃ catalyst at 300°C



Appendix B3.2: CH₄, CO₂ and NO_x gas concentration graphs for all NO concentration over Pd/Al₂O₃ catalyst at 400°C



Appendix B4.1: CH₄, CO₂ and NO_x gas concentration graphs for all NO concentration over Pd/ZSM-5 catalyst at 300°C



Appendix B4.2: CH₄, CO₂ and NO_x gas concentration graphs for all NO concentration over Pd/ZSM-5 catalyst at 400°C

